Evolution of human commensalism in *Passer* sparrows

Effects on skull morphology and brain size

Marina de la Cámara Peña

Master of Science Thesis

Spring 2019

Centre for Ecological and Evolutionary Synthesis

Department of Biosciences

Faculty of Mathematics and Natural Sciences

University of Oslo

Evolution of human commensalism in *Passer* sparrows

Effects on skull morphology and brain size

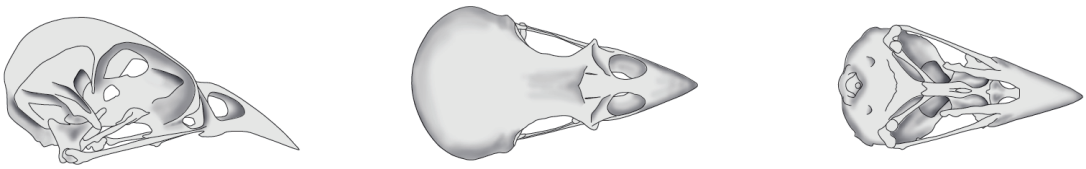

Marina de la Cámara Peña

2019

Evolution of human commensalism in *Passer* sparrows – effects on skull morphology and brain size

Marina de la Cámara Peña

http://www.duo.uio.no/

Trykk: Reprosentralen, Universitetet i Oslo

Acknowledgements

This master thesis was written at the Centre for Ecological and Evolutionary Synthesis (CEES), at the Department of Biosciences, University of Oslo, under the supervision of Dr Mark Ravinet and Prof Glenn-Peter Sætre.

I cannot be more grateful to Mark, for having supervised this thesis and committed to it since the very first moment. Thanks for sharing all your knowledge, ideas and enthusiasm with me, and for your invaluable support as a mentor. It will be difficult for future supervisors to inspire me more than you did. Thanks to Glenn for letting me take part in the sparrow group, for his trust and interest, and for giving me independence to develop this project.

Thanks to the rest of the sparrow group: Ingvild, Åsta, Camilla and Helene, for being not only great company in the field, but also a safe place for support and friendship. To Melissah for the bird training and help, to Angelica for her support and interest in this thesis and to Fabrice for his comments on the manuscript. I am especially thankful to Øyvind Hammer, for training me in the use of the microCT scan, for his availability and advice. To my office mates: Linn, Pernille, Lilja and Elke, for all the hours spent together and the constant support. Full credit to Alexandra Torres for creating the coolest figures of skulls. Thanks to Mohammed, my best neighbour and friend.

Last but not least, special acknowledgement to my family. To my parents, I will never thank you enough for always being my strongest support. *Cuidaremos los unos de los otros, aunque estemos lejos.* I also thank the rest of my family for always being there, especially my aunt Nuria for the continuous inspiration and motivation. Thanks for everything Joël, you are, and will always be, part of my family *pase lo que pase*. Thanks to Elena, David and my bio-people (Clara, Esther, Sara, Ana and Pablo) for being my anchors.

Abstract

Human activities have historically influenced the evolution of other species. Dramatic modifications in land-use and extreme urbanization have increased not only the amount of species associated with human environments, but also the intensity of interaction among them. Hence, the evolution of these organisms can lead us to gain a deeper understanding of our own history.

House sparrows (*Passer domesticus*) are a passerine bird species distributed worldwide due to their close association with anthropogenic environments. The species likely spread from the Middle East, with the advent of the Neolithic revolution less than 10Kya. This shift towards highly variable rural and urban niches has driven a change in diet preferences (mainly based on cultivated cereals such as wheat and barley), which has potentially triggered differences in skull morphology and biting mechanical advantage. Their adaptation to these unpredictable environments may be also reflected in an increase of relative brain size and signatures of selection for genes associated with skull morphology.

In this project, we used 3D geometric morphometric approaches based on microCT scans to study skull morphological adaptations to anthropogenic niches in European and Iranian house sparrow subspecies, Spanish, Italian and tree sparrows. We used the subspecies *P. domesticus bactrianus* as a proxy of ancestral non-commensal ecology. Biting mechanical advantage was calculated to study feeding performance and relative brain size was examined to test whether larger brains tend to develop in commensal species. In addition, we performed genome scans in order to look for signatures of selection of candidate genes associated with craniofacial morphology.

We identified significant differences in skull morphology and relative brain size between commensal and non-commensal groups. Estimates of biting mechanical advantage calculations showed a slight trend towards a more forceful bite in commensal species. At the genomic level, we detected strong signatures of selection for two candidate genes, which play a role in beak depth and length and craniofacial morphology. All these differences between commensals and non-commensals may shed light in understanding the adaptation of house sparrows to human-made environments.

Table of contents

1. Introduction

Human activities have historically had a large impact on the evolution of other species. Good examples include disease organisms, species of commercial interest, invasive species and commensals (Palumbi, 2001). Industrial melanism, herbicide resistance, tolerance to heavy metals, (reviwed by Reznick & Ghalambor, 2001), gut flora (Hooper & Gordon, 2001) and dog domestication (Larson & Fuller, 2014) are well-known cases of adaptation to human environments through artificial and natural selection. As a result, humans and other species might establish different relationships depending on their interaction mechanisms, such as parasitism, mutualism and commensalism (Krebs, 2013). The study of human commensals is therefore interesting because these organisms, via natural selection, have been able to occupy spaces that we modified for our own habitability (in contrast to examples of evolution by artificial selection such as dog and livestock domestication). They are not only a consequence of these modifications but also act as a bioproxy (Jones, Eager, Gabriel, Jóhannesdóttir & Searle, 2013) of large-scale human events (e.g., settlements, colonisations, industrialization and changes of habits). For instance, house mice, a species tightly associated with human settlements, appears to be a good bioproxy to understand Viking movements towards the northern and western British Isles, as they were transported in Viking ships during the Norwegian Viking expansion (Searle et al., 2008).

The term commensalism comes from the Latin "commensalis", which means, literally, "at table together". In biology, commensalism can be defined as an interspecific relationship in which one species (the commensal) obtains benefits such as food, shelter, or locomotion from another species (the host) without causing adverse effects (Mougi, 2016). Consequently, a dependency relationship may be generated between the commensal and –in this case-, the anthropogenic environment.

Although it might seem straightforward to assume that anthropogenic environments are very stable, these niches (both urban and agricultural) turn out to be highly variable (Hulme-Beaman, Dobney, Cucchi & Searle, 2016). This variability and unpredictability appears to be the primary source of selective pressures, such as changes in food availability due to harvest, storage, trade and sudden food waste depletion. Despite greater food availability and buffered seasonal changes in urban environments, these unpredictable and dramatic variations might lead to

sudden population decreases. In agricultural environments, these selective pressures can also be problematic. Although seasonal changes have a more cyclic character and hence might be more predictable, fluctuations appear to be much more intense than in natural habitats (fig. 1.1). Organisms that achieve fixed populations densities despite fluctuating environments might develop higher plasticity in terms of feeding, mating or nesting (Hulme-Beaman et al., 2016).

The home range and feeding resources of both commensals and anthropodependents may be fully or partially anthropogenic. However, the distinction between the two is that commensals are able to compete in natural environments, whereas the survival of anthropodependents is completely conditioned on a human niche (Hulme-Beaman et al., 2016).

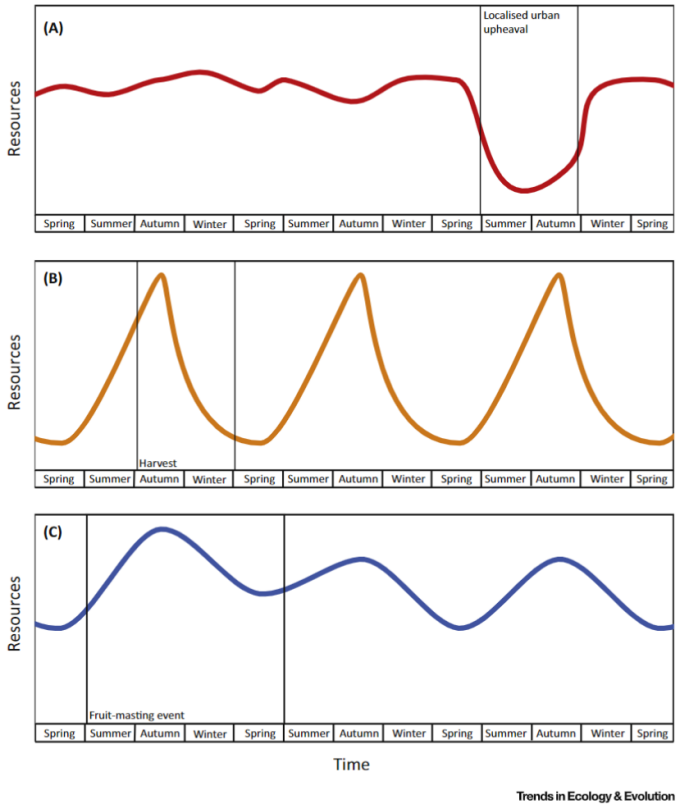

Figure 1.1. Fluctuating resource availability in different environments. (A) Urban, (B) Agricultural, (C) Natural. Taken from Hulme-Beaman et al., 2016. Note the sudden resource depletion in A and the increased fluctuation in resource availability in B.

The house sparrow is one of the most emblematic examples of human commensal species. It can be considered anthropodependent according to Hulme-Beaman et al. (2016) classification, since it would probably go locally extinct if humans abandon an area (Summers-Smith, 1963; Anderson, 2006; Sætre et al., 2012). The house sparrow (*Passer domesticus*) is a passerine bird

species distributed worldwide thanks to its close association with humans. Its native distribution is extended through Eurasia and some areas in the north of Africa, although its range limit towards Eastern Asia remains unclear. House sparrows have also established successful invasive populations in Southern Africa, Australia, New Zealand and the American continents due to later introductions in the 19th and 20th centuries (Summers-Smith, 1988).

The sparrow human-commensalism likely has a single origin in the Middle East with the advent of the Neolithic revolution less than 10,000 years ago (Sætre et al., 2012), giving rise to different subspecies. Summers-Smith (1988) was very interested in the evolution of the sparrow, and gave a reasonable description of these subspecies, mostly based on Vaurie's (1956) distinction in two groups: the *domesticus* (or Paelarctic) and the *indicus* (or Oriental) group (fig. 1.2). The *domesticus* group includes larger birds, with grey cheeks and underparts and occurs in the Palearctic region, whereas the *indicus* subspecies are smaller, with white cheeks and underparts, generally more colourful on the upperparts. Both the phenotypic and geographical distribution of these two groups would suggest that human commensalism originated independently on both groups.

Nevertheless, Summers-Smith himself recognized that this taxonomical classification – merely based on colour and several proxies of size – has many difficulties, since their ranges seem to overlap and hybridization might be occurring. Sætre and colleagues concluded that both groups cluster together (and hence there is no population structure) when mitochondrial and nuclear DNA were analysed, suggesting a recent population expansion. This is consistent with a single origin of human commensalism (Sætre et al., 2012) and subspecies differentiation in this system must therefore be treated with caution.

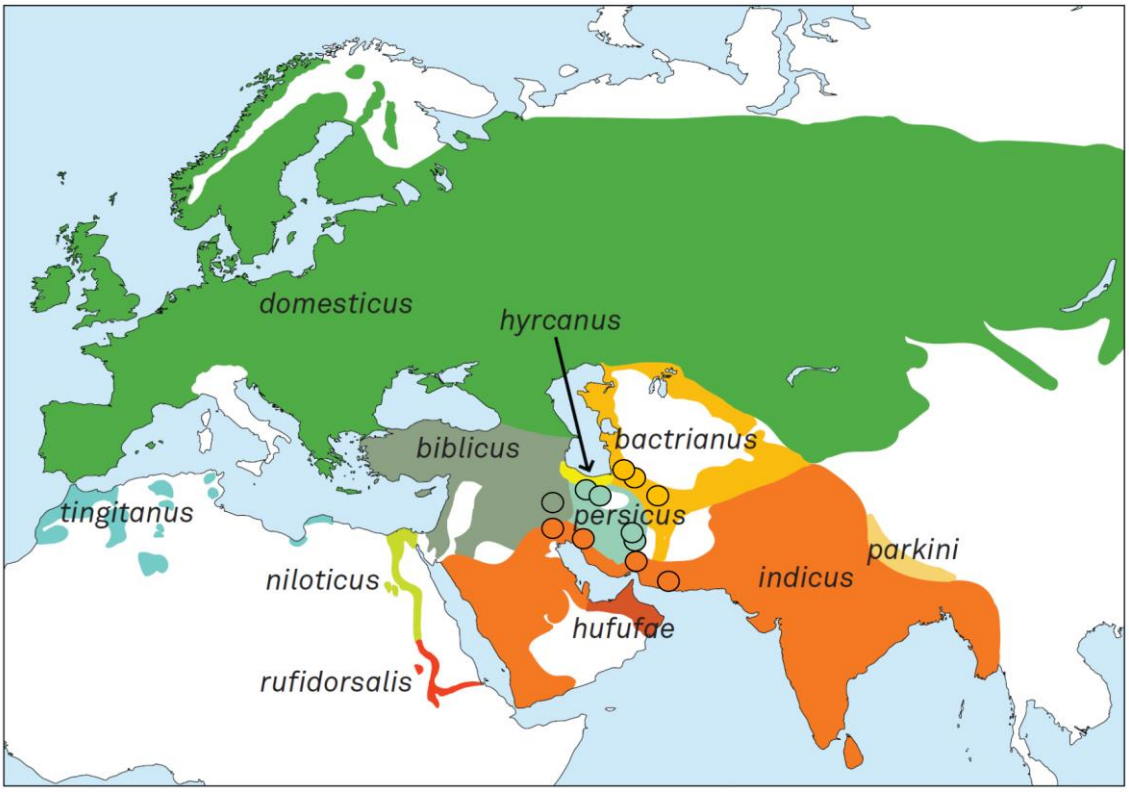

Figure 1.2. Geographical distribution of the different subspecies of house sparrow. Cold colours and warm colours represent the *domesticus* group and *indicus* groups, respectively. Outlined points indicate sampling locations for the subspecies of Iranian house sparrow used in this project: *P.d. bactrianus, biblicus, indicus* and *persicus*. Species distributions might vary between authors. Modified from Sætre et al., 2012.

However, in Central Asia, the subspecies *P. domesticus bactrianus* (hereafter Bactrianus sparrow, which belongs to the *indicus* group) appears to have retained the ancestral wild type ecology, and it is the only subspecies that migrates, according to Summers-Smith observations (Summers-Smith, 1988). Despite the overlap in its range distribution with *P. d. persicus* in western Afghanistan and with the house sparrow in Kazakhstan, Bactrianus does not seem to interbreed with any of them, indicating an important split between this subspecies and the others (Gavrilov & Korelov, 1968).

A recent study using whole genome resequencing data (Ravinet et al., 2018) suggested that the divergence between the Bactrianus and the house sparrow occurred 11.1 Kya, prior to the invention of agricultural technology, and the house sparrow likely spread into Europe around 6Kya with early agricultural societies. This means that Bactrianus might actually represent a relict population of the ancestral wild house sparrow. In addition, this is well supported by population structure analyses and signatures of selection in the house sparrow for genes that

appear to be related to craniofacial development and adaptation to a starch rich diet; both of which might be associated with commensal activities. Thus, a necessary next stage is to properly characterize phenotypic variation among species – i.e. skull morphology, beak shape and bite force.

Ecologically, whereas all the other subspecies live in human altered habitats and feed from human food waste, Bactrianus is found in mesic habitats, feeding on wild grass seeds, which are smaller and less encapsulated than those from cultivated crops. Unlike human-commensal house sparrows, it is migratory, wintering in the southwest of India and Pakistan (Summers-Smith, 1988). In birds, urban exploiters such as commensal house sparrows appear to differ in social structure; they are more gregarious and sedentary (i.e., they do not migrate), and their diet tends to be less insectivorous (Kark, Iwaniuk, Schalimtzek & Banker, 2007).

Essentially, the shift to an agriculturalist sedentary life style in human societies in Western Asia opened a new environment for other species to colonize (Fuller & Stevens, 2019). In humans, this can be considered a form of cultural niche construction, since it implicates processes such as culturally transmitted practices, long-term modifications (i.e., soil clearance) and genetic evolution of both directly domesticated organisms in crops and the species which became associated with them (Fuller & Stevens, 2019). Nonetheless, species such as house sparrows are likely to have changed their diet to this new kind of seed: larger, with rapid germination and higher caloric value and without specialised dispersal mechanisms, although this enlargement might have arisen without previous deliberation by early farmers (Kluyver et al., 2017). Consequently, it is likely that this event generated certain selective pressures, which have driven the evolution of differences on beak and skull morphology in commensal sparrows. Thus, human commensal house sparrows have apparently evolved to handle the tougher and encapsulated cultivated grass seeds such as wheat and barley and have larger beaks and more robust skulls than Bactrianus. Additionally, body size differences are noticeable between both ecologies, with commensal birds being bigger than non-commensal (Riyahi et al., 2013).

Besides changes in structures directly related with resource consumption, these selective pressures might have played a role in other traits too. For instance, relative brain size has also shown variation in terms of human niche adaptation in birds. It seems that birds tend to evolve a larger brain size when they invade regions with high environmental variability –characteristic of human agricultural societies- (Sayol et al., 2016), novel environments or when they are exposed to situations when feeding innovation is key for survival (Sol, Duncan, Blackburn,

Cassey & Lefebvre, 2008). It has been suggested that relative brain size is also related to sedentary rather than a migratory ecology (Sol, Lefebvre & Rodríguez-Teijeiro, 2005). Moreover, larger relative brain sizes are positively correlated with the proportion of urban dwellers of multiple families of passerines (Maklakov, Immler, Gonzalez-Voyer, Rönn & Kolm, 2011). Hence, these traits are likely to occur in human commensal species (in birds, Møller et al., 2015; in mammals, Santini et al., 2019).

Other *Passer* species show variation in their associations with humans. The tree sparrow (*P. montanus*) is known to be less associated with humans than the house sparrow, as well as the Spanish sparrow (*P. hispaniolensis*), although the latter is 'more commensal', at least in Europe (Summers-Smith, 1988). Spanish sparrows are present across the Mediterranean and in the Middle East, and they appear to have admixed with house sparrow populations when the latter expanded into Europe (Ravinet at al., 2018). This also likely gave rise to their hybrid, the Italian sparrow (*P. italiae*). The hybrid species occupies Italy and some Mediterranean islands, and lives in both allopatry and sympatry with its Spanish parental (fig. 1.3). Ecologically, Italian sparrows resemble the commensal subspecies of house sparrow (commensal ecology), although they exhibit genomic and phenotypic mosaicism from its parental species (Elgvin et al., 2017).

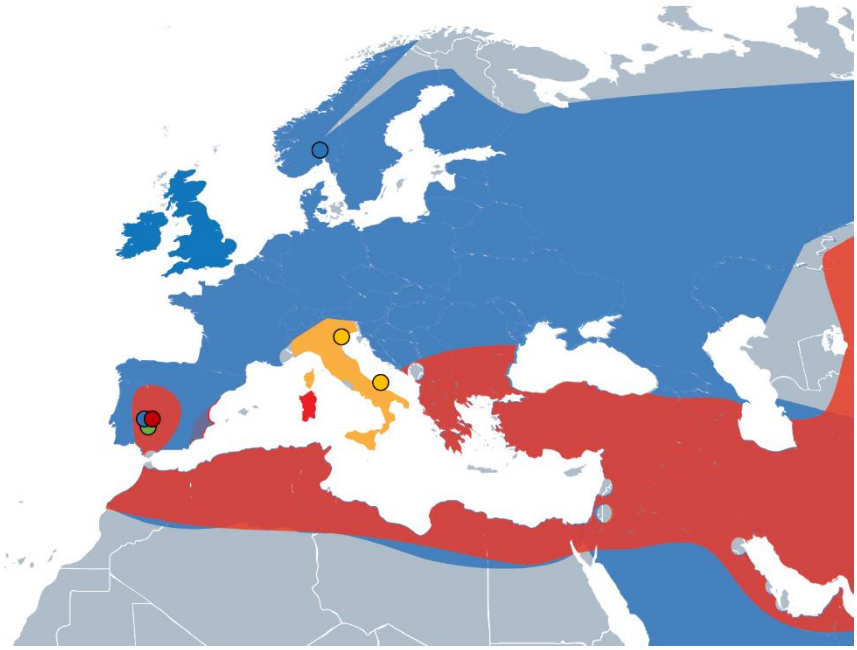

Figure 1.3. Geographical distribution and sampling locations (outlined points) of house (blue; *P. domesticus domesticus*), Italian (yellow; *P. italiae*) and Spanish (red; *P. hispaniolensis*). Darker red represents the distribution overlap of house and Spanish. The green point is the location where F1 hybrids were sampled (i.e., captive bred Spanish x house).

1.1. Aims

The *Passer* sparrow system is an intriguing scenario to compare multiple species with different levels of human association, in the framework of a well-understood evolutionary history. The agricultural shift in European societies, driven by the Neolithic revolution and the subsequent selective pressures have likely triggered a series of changes in these species, which are worth studying in terms of genomics, geometric morphometrics, biomechanics and behaviour.

Therefore, we raise the following questions: has the shift in diet towards cultivated cereals such as wheat and barley led to a change in the skull morphology of commensal house sparrows? Is this change reflected at different levels of commensalism? Does this have an effect on biting performance? Do commensals present enhanced encephalization as an adaptation to highly variable environments? What is the role of genes traditionally associated with craniofacial and beak development in this scenario?

Here, we aim to characterise skull morphological divergence using 3D morphometrics, among house (i.e., from Europe and Iran, including the wild commensal *P. domesticus bactrianus*), Spanish, Italian and tree sparrows and address differences in biting mechanical advantage and relative brain size. Additionally, we perform genome scans in order to find signatures of selection for candidate genes associated with craniofacial morphology in birds.

2. Material and methods

2.1. Specimens

A total of 86 skulls of adult European house sparrows (*Passer domesticus domesticus*) and Iranian house sparrow subspecies *P. d. bactrianus, P.d. biblicus, indicus* and *persicus*, from several locations in Iran were used for this project. We also added Spanish (*P. hispaniolensis*), Italian (*P.italiae)*, and tree sparrows (*P. montanus*) to the analyses (table 2.1). Artificially hybridised Italian sparrows – namely F1 hybrids - were also included. Although we had a few *P. d. hyrcanus* skulls we decided to exclude them from the analysis because they were partially broken.

The Iranian specimens were obtained from different museum and university collections in Iran. Wild, free-living house sparrows from Oslo were trapped using mist nets in the Botanical Gardens of the Natural History Museum (University of Oslo) during the spring of 2016 (3rd – 6th May), under license (license number 1236, Melissah Rowe) and with permission to euthanise and sample skulls (2016/2225) from Miljø-Direktoratet. House and Spanish sparrows from Spain (wild, free-living and trapped with mist nets) and F1 hybrids (bred in captivity and raised in aviaries) were sampled near Olivenza (Badajoz) on 28th March 2017, and processed at the University of Extremadura. Trapping and sampling of these birds was conducted in accordance with the Spanish Animal Protection Regulation RD53/2013 and methods were approved by the Institutional Commission of Bioethics at the University of Extremadura (CBUE 49/2011). Wild, free-living Italian sparrows were trapped with mist nets 22km away from Padova on 22nd June 2017, with permits issued by the Istituto Superiore per la Protezione e la Ricera Ambientale (ISPRA), license no. 233240 (decreto 90) to Matteo Griggio. Italian sparrows from Puglia were trapped wild, free-living, under permits by the ISPRA, decreto 207/2015 of the Regione di Puglia, licence no. 337 to Glenn-Peter Sætre. All these birds were killed by cervical dislocation. Skulls were prepared by submerging in a water and enzyme powder (Bio Tex) mix and incubating at 46 degrees C for 2 - 4 weeks. Once all tissue had been dissolved, clean skulls were washed in hot water and dried on paper for 48 hours.

Table 2.1. Species and subspecies used, location by region (and country) and sample size, divided by males (m), females (f) and unknown (NA).

Species or subspecies	**Location**	**Sample size**	
House	Oslo (Norway)	8	4m, 4f
Passer domesticus	Badajoz (Spain)	3	3m
		11	**7m, 4f**
Spanish	Badajoz (Spain)	**3**	**3f**
Passer hispaniolensis			
Italian	Foggia (Italy)	10	5m, 5f
Passer italiae	Padua (Italy)	3	3f
		13	**5m, 8f**
F1 Hybrid	Badajoz (Spain)	**10**	**5m, 5f**
P. domesticus x hispaniolensis			
Bactrianus	Govareshk (Iran)	6	4m, 2f
Passer domesticus bactrianus	Bojnord (Iran)	2	2f
	Mashhad (Iran)	1	1f
		9	**4m, 5f**
Biblicus	Kermunshah (Iran)	**6**	**4m, 2f**
Passer domesticus biblicus			
Indicus	Bushehr (Iran)	2	2f
Passer domesticus indicus	Chabahar (Iran)	1	1f
	Dezful (Iran)	2	1f, 1NA
	Minab (Iran)	1	1m
		6	**1m, 4f, 1NA**
Persicus	Baft (Iran)	3	2m, 1f
P. domesticus persicus	Kuhbanan (Iran)	2	1f, 1NA
	Shahr-e Rey (Iran)	10	9m, 1NA
	Shahr-e Qods (Iran)	4	1m, 3NA
		19	**12m, 2f, 5NA**
Tree	Mashhad (Iran)	5	2m, 2f, 1NA
Passer montanus	Goosh village (Iran)	2	2NA
	Kashmar (Iran)	2	2NA
		9	**2m, 2f, 5NA**
Total		**86**	**40m, 35f, 11NA**

2.2. Skull morphology

2.2.1. microCT scanning and landmarking

86 samples were scanned with the use of a high-resolution X-ray microCT scanner Nikon XT H 225 ST. Scans were conducted at the Natural History Museum of Oslo (Norway), using 85kV and 300µA. 17 samples were scanned at 55kV and 300µA because of technical problems, but this did not affect the quality of the scans or the placement of landmarks.

Throughout this procedure, the scanner creates a set of cross sectional images, which are much more detailed than regular X-ray images. A detector placed opposite to the X-ray source receives these images (fig. 2.1). We optimized the scans using 3016 projections (images) and taking one frame per projection only (to minimize scanning time) and an exposure time of 1000ms. Skulls are continuously rotated while each projection is being taken and this generates the appearance of ring artefacts, mainly on the dorsal area of the braincase. However, this did not significantly affect the quality of the scans and was barely visible in all cases, so we decided not to minimise such artefacts. The resulting .TIF images were computed into three-dimensional reconstructions for each skull. .VOL files were rendered, visualized and analysed using Avizo 9.1.0.

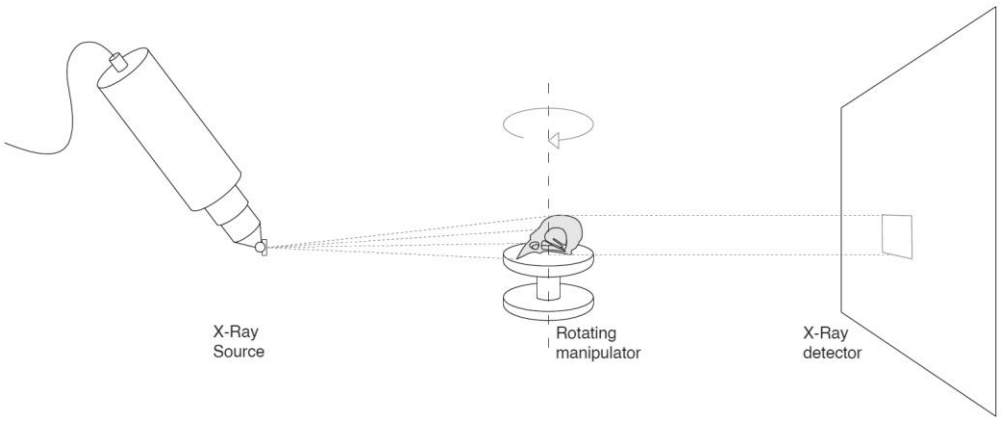

Figure 2.1. microCT scan diagram. The source emits X-rays towards the sample, which is continuously rotating. The X-ray detector captures each cross-sectional image (projection). These projections are then compiled and processed for later 3D reconstruction.

20 landmarks in three-dimensional space were digitalized three times in Avizo for each individual and their mean was used for the analysis of coordinates (fig. 2.2). Although landmarks were taken on both sides of the skull, we decided to use those on the right side only (arbitrarily chosen) and on the sagittal plane, since all the skulls were largely symmetrical and our question was not focused on assessing asymmetry in cranial morphology. Placing landmarks on one side only avoids shape redundancies and hence, simplifies statistical analysis since the total number of variables is reduced and the number of degrees of freedom is not inflated (Zelditch, Swiderski, Sheets, & Fink, 2004).

Outline curves and surface analysis were not implemented in this study, since landmark coordinates represent discrete anatomical locations that are able to describe biological traits of interest (reviewed by Adams, Rohlf & Slice, 2013). Also, landmarks do not alter their position due to other landmarks, can provide adequate coverage of the morphology and can be found repeatedly and reliably (Zelditch et al., 2004). For this reason, multiple sets of landmarks were tested in order to optimize the analyses (i.e., maximising shape variation, minimising uninformative variables and accounting for traits that concern our study question).

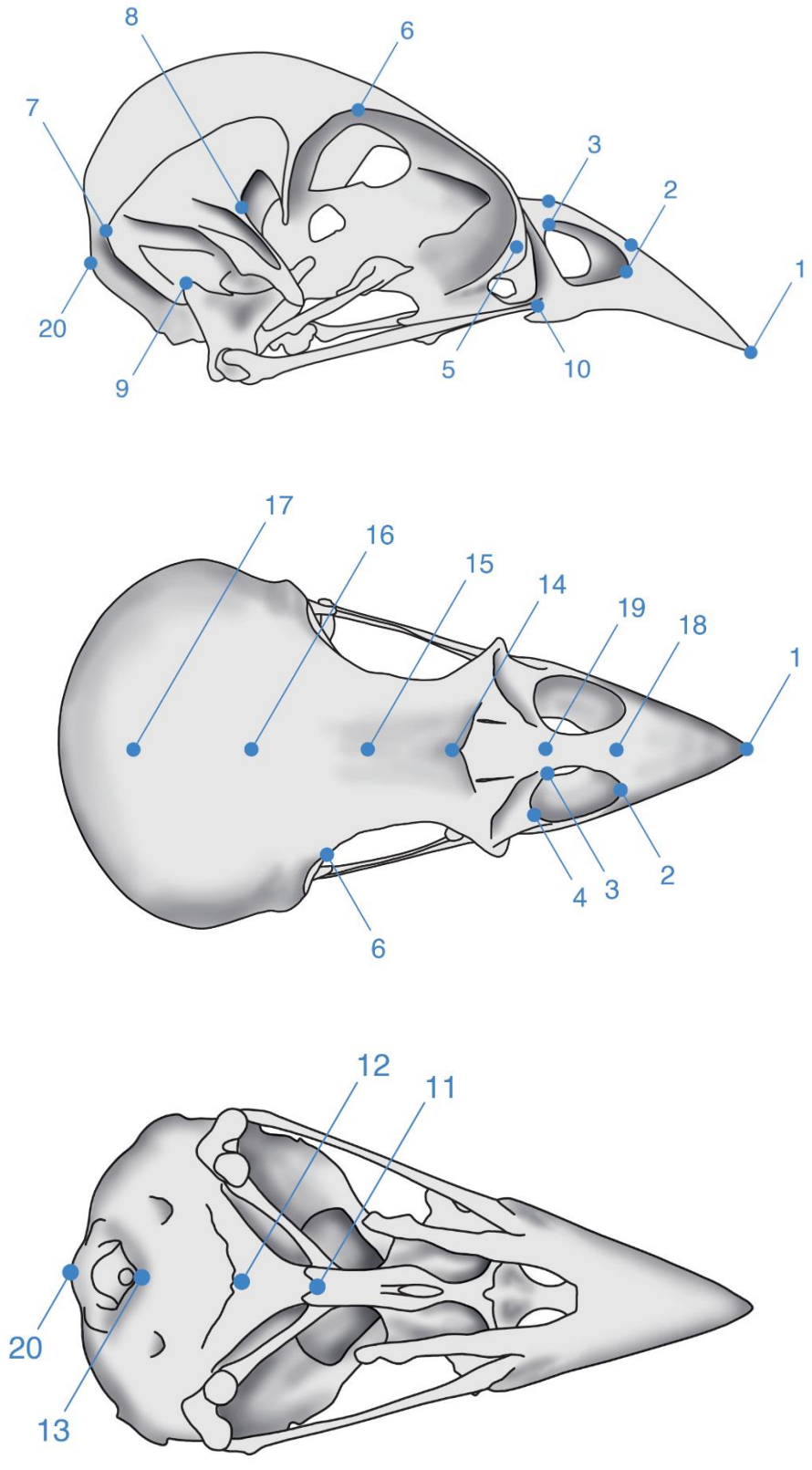

Figure 2.2. Landmark configuration. Landmark description and a more detailed figure of non-obvious landmarks can be found in the appendix (A1).

2.2.2. Partial Generalized Procrustes Analysis

Landmark coordinates were sorted in a 3D array in R and Partial Generalized Procrustes Analysis (Gower, 1975) was implemented with the *gpapgen()* function in geomorph (Adams, Collyer & Kaliontzopoulou, 2018). Each landmark configuration is translated (so each configuration has the same centroid), scaled (centroid size for each configuration will be equal to 1.0) and rotated (to minimize Procrustes distance). All configurations are then superimposed in the tangent space. Consequently, shape can be defined as all the geometric features present in a landmark configuration except for scale, location and rotation effects (Kendall, 1977). Size is now, by definition, mathematically separated from shape and is defined by centroid size, which is the square root of the sum of squared distances of a set of landmarks from their centroid.

2.2.3. Allometry

Since Procrustes superimposition defines shape and size as different variables, it is important to study whether there is covariation between them (i.e. presence of allometry), according to the Gould-Mosimann school. This line of thinking states that size and shape are conceptually and mathematically separated and hence, can be studied as different variables, in opposition to the Huxley-Jolicoeur school, which defends the idea that each shape variable contains size information and both concepts are indivisible (reviewed by Klingenberg, 2016).

In order to detect significant effects of size on shape, a multivariate regression was performed. Procrustes data was set as the independent variable and centroid size, species and sex as dependent variables in the model. For these analyses, the geomorph functions *procD.lm()*, *advanced.procD.lm()* and *procD.allometry()* were used. An ANOVA type I (sequential) test with randomized residual permutation procedure (1000 permutations) was conducted for model selection and a homogeneity of slopes test (HOS) to study allometric trajectories was performed. *procD.lm()* compares two models with nested variables. We tried different combinations of the following variables: size, logsize, species (grouping variable), sex and their interactions.

2.2.4. Principal component analysis

Out of the 60 shape variables (20 landmarks in three dimensions), degrees of freedom were reduced to 53 during Procrustes superimposition. In order to define the pre-shape space, three dimensions were lost in translation (since we are using 3D coordinates) and one in scaling (we fix centroid size for each configuration to 1). After rotation, three additional dimensions were lost, and our final number of dimensions of shape space will be $3 \times 20 - 3 - 1 - 3 = 57$. Principal components analysis (PCA) was then performed on the Procrustes data using base R functions. Shape changes along the most relevant eigenvectors were visualized using wireframes both in 2D and 3D, using rgl R package (Adler & Murdoch 2018).

Allometry-corrected PCA was also performed to explore the Procrustes residuals shape space. To explain significant shape differences between groups multivariate linear regressions were conducted for the first 10 dimensions of the allometry-corrected PC scores and MANOVA analyses were used to detect overall differences.

We used subsets of landmarks of the beak and the rest of the skull separately to study their centroid size and their relationship as different functional structures. 8 landmarks were used for the beak (1, 2, 3, 4, 10, 14, 18 and 19) and 12 for the rest of the skull (5, 6, 7, 8, 9, 11, 12, 13, 15, 16, 17, 20) (see fig 2.2).

2.3. Biting mechanical advantage

Biting mechanical advantage (MA) of the jaw closing is a measure of efficiency where force is transferred from the masticatory muscles through certain structures of the cranium to the food. This calculation arises from the need to link form and performance (Dumont et al., 2014), meaning that we are able to correlate changes in skull morphology with a measurement of bite force.

MA calculations are derived from lever mechanics, and estimate the force transmission of a first class lever in which the moment arm of the muscle (the effort) is the input force and the

moment arm of the biting (the load) is the output (Westneat 1994, Sakamoto 2010). The resulting MA is then the ratio between the length of the input arm and the length of the output arm (see eq. 2.1).

$$MA = \frac{effort}{load} = \frac{length\ input\ arm}{length\ output\ arm} = \frac{d(fulcrum, m.AMEM/S)}{d(fulcrum, tip\ beak)}$$

Equation 2.1. Biting mechanical advantage (MA) formula used in this system

This system has been previously used to measure mechanical advantage both in fish (Westneat, 1994) and birds (Navalón, Bright, Marugán-Lobón & Rayfield, 2019). Since the main mandibular adductor muscle in birds is the m. adductor mandibulae externus medialis/superficialis (m.AMEM/S) (Lautenschlager, Bright & Rayfield, 2014), the input arm of the lever goes orthogonally from a linear proxy of this muscle group to the most ventral tip of the quadrate (where it meets the lower jaw), which is the fulcrum of the lever (fig 2.3). The output arm goes from the fulcrum to the tip of the beak. This is because it is the primary structure in contact with food, it is uncertain where to set other points on the margin of the beak, and the tip of the beak and a midpoint between the tip and the end of the premaxillary structure have shown high correlation in previous studies (Navalón et al., 2019).

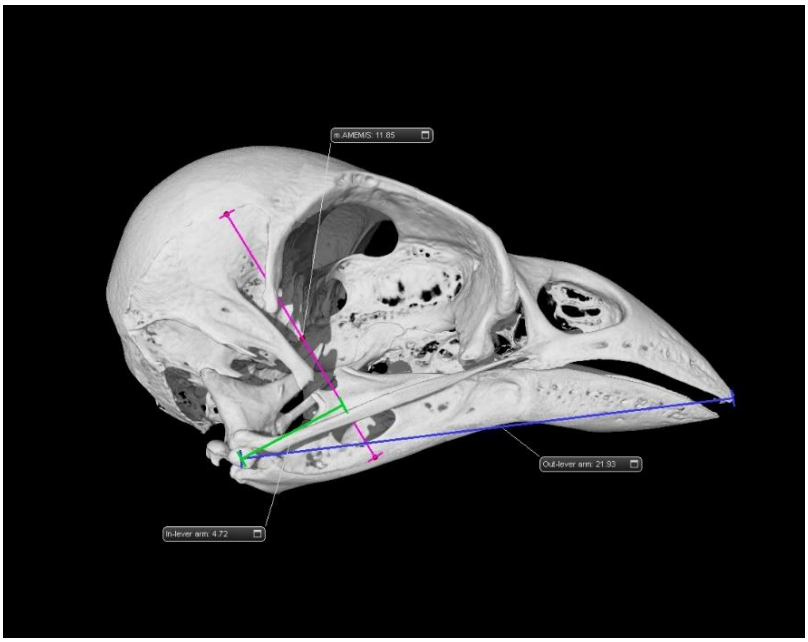

Figure 2.3. Example of the lever system used to calculate biting mechanical advantage. Image extracted directly from Avizo. The pink line is a proxy of the m.AMEM/S, green represents the in-lever arm and blue the out-lever arm. The point where blue and green meet is the fulcrum.

Unfortunately, biting MA could only be calculated for only 26 out of a total of 86 skulls, because the quadrate bone was not present in the majority of samples. The measured specimens include House (n=9), Spanish (n=2), Italian (n=11) sparrows, and F1 hybrids (n=4).

A Kruskal-Wallis test was used to infer differences in mean between groups and Levene's test was performed to assess variance differences. Kruskal-Wallis is a non-parametric test that performs a rank based one-way ANOVA. Levene's test is a variance test for more than two groups that does not assume normality either. This test was performed with the *car* package in R (Fox & Weisberg, 2011).

2.4. Braincase volume

Skulls were weighed separately using a precision scale (Sartorius ED224S – Sartorius AG Germany) adjusted to the nearest 0.001g. Braincase volume was then measured by filling each skull with mustard seeds through the foramen magnum or the orbit (if the foramen magnum was too narrow), blocking the remaining orifices with tape and weighing the filled skull. Skulls were tapped multiple times during the filling process to ensure seeds were compacted. Each skull was filled and weighed five times to correct for measurement errors (± 0.00828g on average). Then, the volume of the seeds was calculated using a 10 ml graduated cylinder. This procedure has been extensively used in the literature: Radinsky (1967) used water and shot in mammals, and methodologically defined *relative brain size.* Falk, Cheverud, Vannier & Conroy (1986) studied primate brain volume using seeds; Mann, Glickman & Towe (1988) with rodents, using gauge shot instead of seeds; and Marino (1998) with cetaceans, using plastic beads. This method has also been implemented with hummingbird skulls (Rehkämper, Schuchmann, Schleicher & Zilles, 1991) and Iwaniuk & Nelson (2002) used lead shot to predict brain mass using the endocranial volume in many bird species, showing a highly significant relationship between both measures

Using the image segmentation tool in Avizo, we also calculated endocranial volumes of 15 randomly picked skulls, in order to ensure that our volumetric method properly accounts for skull volume. The volume file was first resampled, increasing the voxel size by approximately

10 (depending on the quality of each scan), to minimize the number of resulting layers to work with. After the endocranial area of each layer was computed, a volume file of the endocranial cavity was obtained. Correlation tests show high concordance between both measurements (but see Validation of methods in the Appendix, A2). Isosurface rendering was used for visualization purposes only.

In order to correct for size effects, tarsus length was used as a proxy of body size. Tarsus length is a skeletal dimension that can predict body size defined in this case as structural size (a reserve-independent measure) (Rising & Somers, 1989; Piersma & Davidson, 1991; Husby, Hille & Visser, 2011; Labocha & Hayes, 2012). A linear regression model between –both log transformed- braincase volume and tarsus length was conducted. Its residuals were studied to account for group differences (similarly, Sol et al., 2005). These analyses were computed with base R functions.

2.5. Genome scans

We used previously published whole genome resequencing data of Bactrianus (n=19), *biblicus* (n=9), house (n=83), *indicus* (n=7), Italian (n=145), *persicus* (n=9), Spanish (n=70) from Elgvin et al. (2017), Ravinet et al. (2018) and Runemark et al. (2018). Tree sparrows were excluded from these analyses because of high levels of differentiation between these and the focal Eurasian species.

Sequence data was aligned to the house sparrow reference genome (Elgvin et al., 2017) and genotypes were called using GATK (3.7) HaplotypeCaller (DePristo et al., 2011). Filtering included calls occurring at all sites (i.e. variant and invariant positions) in at least 80% of individuals, with a genotype quality of Phred=20, a minimum depth of 5x and a maximum of 20x. Filtering was performed using vcftools 0.1.13 (Danecek et al., 2011) and bfctools 1.1 (Danecek & McCarthy, 2017). Further details of the filtering process can be found in Ravinet et al., 2018.

We chose 50 candidate genes related with skull and beak morphology in birds to explore whether they have played a role in adaptation to a human commensal niche recent adaptation to human commensalism has had an effect on them. bcftools 1.9 (Danecek & McCarthy, 2017) was used to extract genotype calls covering the genes. Subsequently, these sequences were read into the R package PopGenome (Pfeifer, Wittelsbürger, Ramos-Onsins & Lercher, 2014) to test for signatures of selection; focusing on nucleotide diversity (Nei & Li, 1979), Tajima's D (Tajima, 1989) and F_{ST} (Weir & Cockerham, 1984). Additionally, we randomly sampled 50 coding genes (hereafter 'null' genes) that did not overlap with the candidate genes, in order to compare their values with the candidate genes.

Briefly, nucleotide diversity (π) can be defined as the average number of nucleotide differences per site between randomly chosen sequence pairs from the population (Π), standardized by sequence length. Tajima's D uses nucleotide diversity to calculate the Tajima's estimator (θ_T), and the number of segregating sites for the Watterson estimator (θ_w). Tajima's D can be therefore defined by the difference between these two, divided by their variance (see eq. 2.2).

$$D = \frac{\pi - s\,/a}{\sqrt{V(\pi - s\,/a)}} = \frac{\theta_T - \theta_w}{\sqrt{V(\theta_T - \theta_w)}}$$

Equation 2.2. Tajima's D, where π is nucleotide diversity, s is the number of segregating sites, a is a normalizing term and V is the variance.

Since the presence of rare polymorphisms increase π, but less so for *s* which is less sensitive to them, Tajima's D will be negative in cases of recent selective sweep or population expansion. On the contrary, Tajima's D will be positive when rare variants are present at low frequencies, which can be interpreted as balancing selection or population contraction. If Tajima's D is close to zero, there is no evidence of selection, and the population in question is expected be evolving in equilibrium.

F_{ST} is also widely used in population genomics. F_{ST} is an index for allele fixation, meaning that it measures the loss of heterozygosity relative to the metapopulation, and can be used as a way to calculate population differentiation. Consequently, F_{ST} will be zero when two populations have equal allele frequency, and will be close to 1 when different alleles are fixed in each population.

The 50 candidate genes were chosen based on the available literature on the genetic architecture of beak shape and craniofacial morphology in birds (Mallarino et al., 2011, Mallarino et al., 2012, Lamichhaney et al., 2015, Lawson & Petren, 2017 in Darwin's finches; Ravinet et al., 2018, Lundregan et al., 2018 in sparrows, and see Appendix A5 for a complete list of genes). Most of these genes have been extensively studied and their function in the development of the premaxilla is known (such as BMP4 in adaptive radiations in vertebrates (finches: Abzhanov, Protas, Grant, Grant & Tabin, 2004; cichlids: Terai, Morikawa & Okada, 2002)). The rest have been described in the flanking regions of SNPs that contribute largely to bill shape and size in house sparrows (e.g.: CBPZ (which plays a role in BMP pathways) is the flanking region of SNP that explains 1.6% in bill depth in a large-scale metapopulation study of house sparrows in Nothern Norway (Lundregan et al., 2018). We further focused on five important candidates genes in beak and skull morphology in birds and studied in more detail their values of nucleotide diversity, Tajima's D and F_{ST} within the set of putative beak candidate genes (see table 2.2).

We performed linear models with base R functions on Tajima's D, nucleotide diversity and F_{ST} to test whether these values significantly differed between gene statuses (i.e., candidate or null) or among populations.

Table 2.2. Five important candidate genes that have a known effect in craniofacial structure and/or beak morphology in birds. A list for the 50 candidate genes can be found in the Appendix A5.

Gene	Chr	Function	Literature
TGFB2	3	Transforming growth factor beta II (*Gallus gallus*). *TGFB2-(receptor)* is involved in the development of premaxillary bone. Expression upregulated for longer and deeper beaks in finches.	Lundregan et al., 2018 Mallarino et al., 2011 (on *TGFB2r*)
ALX1	1A	ALX homeobox 1 (*Homo sapiens*). Encodes a transcription factor that affects craniofacial development mesenchyme and the first pharyngeal arch. Associated with beak shape diversity in finches.	Lamichhaney et al., 2015 Uz et al., 2010
FZD1	2	Frizzled-1 (*Gallus gallus*). Associated with bill morphology. It belongs to the WNT pathway. Expression upregulated in wider beaks.	Brugmann et al ., 2009 Lundregran et al., 2018;
Col11a1	8	Collagen alpha-1(XI) chain (*Mus musculus*) Regulates craniofacial and skull development. Associated with Marshall's syndrome in humans (skull thickness and abnormal facial structure)	Griffith et al., 1998 Ravinet et al., 2018
BMP4	5	Bone morphogenetic protein 4 (*Gallus gallus)*. Development of prenasal cartilage. Expression upregulated for deeper and wider beaks in finches.	Abzhanov et al., 2004 Mallarino et al., 2011

3. Results

We found differences in skull morphology using 3D geometric morphometrics approaches between groups, potentially associated with commensal and wild type ecologies. We also found significant differences in relative brain size between these groups and a clear trend when studying biting mechanical advantage in a subset of species. Additionally, we detected strong signatures of selection for two candidate genes, which play a role in beak depth and length and craniofacial morphology.

3.1. Skull morphology

The PCA of variation in allometry-corrected skull shapes reveals that the first ten dimensions (out of 57) explain most of the shape variance (74.92%, see variance contributions in Appendix, A4.1). Particularly, the first PC accounts for 16.15% of the variance and the second for 12.83% (almost 30% of the total variation, fig. 3.1 a). Since variance contributions of the first 10 PCs decrease very gradually (see scree plot in Appendix, A4.2), we focused subsequent analyses on these axes in order to find biologically relevant shape differences at both inter and intraspecific level. Only the first two dimensions are shown (in PCA, fig 3.1; linear models, tables 3.1 and 3.2) because they explain the most relevant and dramatic changes in skull morphology and group separation is more evident. Other dimensions tend to account for intraspecific variability that will be discussed later on.

(a)

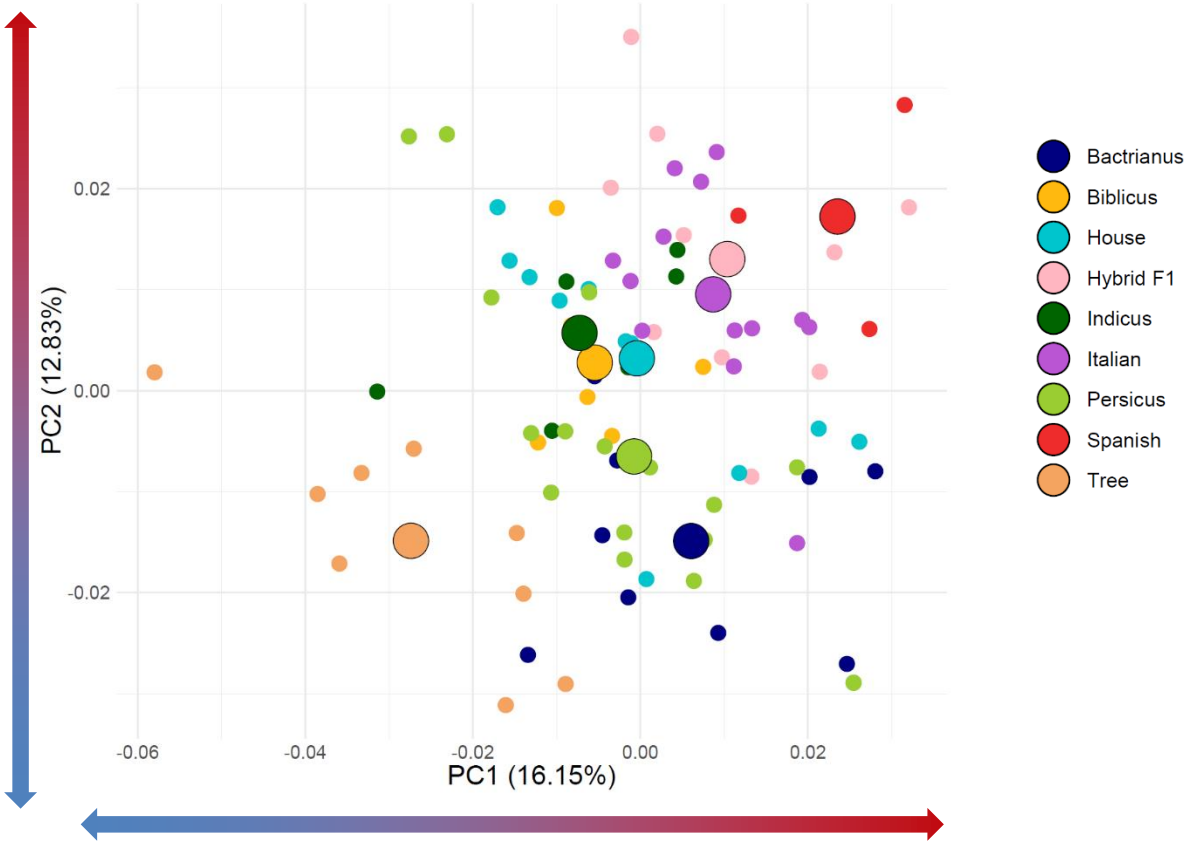

(b)

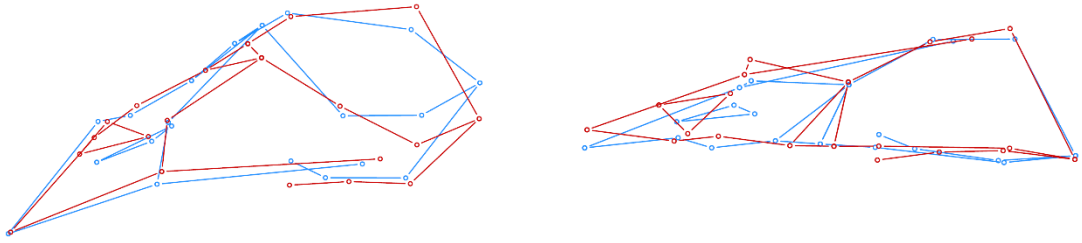

PC1 shape changes (amplified x1.5)

(c)

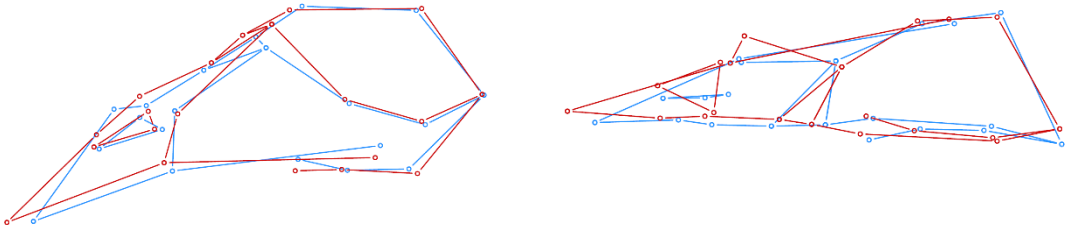

PC2 shape changes (amplified x1.5)

Figure 3.1. (a) PCA on allometry-free Procrustes distances showing species distribution along PC1 and PC2 for skull shape variation. Each point represents one individual. Large and outlined points represent mean shape per group (i.e. species or subspecies). Non-allometry corrected PCA is shown in the Appendix A4 (fig. A4.2) with a table of proportion of variance explained of the first 10 PCs (table A4.2) and scree plot (fig. A4.3).

Wireframes represent predicted extreme shape changes (exaggerated to 1.5x) along the axes. The lowest value both in PC1 (b) and PC2 (c) is represented by the blue wireframe, and the highest value is depicted in red (arrows at the margins of the PCA also explain this, for easier visualization). Possible unnatural deformations (like an almost inexistent nostril in c, dorsal view) are due to 1.5 amplification of the wireframes

PC1 essentially separates the outgroup from the study group, placing Spanish sparrows at the opposite extreme of this axis. The tree sparrow (outgroup) has both low PC1 and PC2 values. PC2 appears to separate groups more clearly, although overlap among them is evident. On this axis, there is a gradient from Bactrianus and tree towards Spanish, passing along *persicus*, the house-*biblicus*-*indicus* cluster and lastly the Italian-hybrid F1-Spanish cluster.

Multivariate linear regressions on the first 10 dimensions of the allometry-corrected PC scores showed that shape is explained by the grouping variable for the first two axes (PC1: $p < 0.0001$, adj. $R^2 = 0.406$; PC2: $p < 0.0001$, adj. $R_2 = 0.4022$). PC1 explains the majority of phenotypic variation between the Eurasian species and the tree sparrow (outgroup). When Bactrianus is set to the intercept, it differs from all other groups except the tree sparrow. PC2 on the other hand, separates the Eurasian subspecies. The rest of PCs account for minor and almost no significant differences (Table 1.1, 1.2).

Table 3.1. Multivariate linear regression on PC1. t-tests are relative to the Bactrianus sparrow. $F_{8, 77} = 8.263$, $p = 65.18 \times 10^{-8}$, adj. $R^2 = 0.406$. Signif. codes: 0 '***' 0.001 '**' 0.01 '*' 0.05 '.' 0.1 ' ' 1

	Estimate	**Std. Error**	**t value**	**Pr (<|t|)**
Bactrianus (int)	0.006057	0.004359	1.389	0.1687
Biblicus	-0.011497	0.006893	-1.668	0.0994 .
House	-0.006475	0.005878	-1.102	0.2741
Hybrid F1	0.004320	0.006009	0.719	0.4744
Indicus	-0.013313	0.006893	-1.931	0.0571 .
Italian	0.002629	0.005671	0.464	0.6442
Persicus	-0.006820	0.005292	-1.289	0.2014
Spanish	0.017472	0.008719	2.004	0.0486 *
Tree	-0.033446	0.006165	-5.425	6.47e-07 ***

Table 3.2. Multivariate linear regression on PC2. . t-tests are relative to the Bactrianus sparrow. $F_{8, 77} = 8.149$, $p = 6.47x10^{-8}$, adj. $R^2 = 0.406$. Signif. codes: 0 '***' 0.001 '**' 0.01 '*' 0.05 '.' 0.1 ' ' 1

	Estimate	Std. Error	t value	Pr (<|t|)
Bactrianus (int)	-1.490e-02	3.899e-03	- 3.821	0.000268 ***
Biblicus	1.767e-02	6.165e-03	2.866	0.005365 **
House	1.809e-02	5.257e-03	3.441	0.000939 ***
Hybrid F1	2.792e-02	5.374e-03	5.195	1.63e-06 ***
Indicus	2.061e-02	6.165e-03	3.343	0.001284 **
Italian	2.443e-02	5.072e-03	4.816	7.16e-06 ***
Persicus	8.375e-03	4.733e-03	1.769	0.080784 .
Spanish	3.214e-02	7.798e-03	4.121	9.43e-05 ***
Tree	1.932e-05	5.514e-03	0.004	0.997213

A MANOVA test on PC values of the first 10 dimensions was performed in order to study group differences, finding a significant group separation ($F_{8, 77} = 2.8039$, $p < 0.001$, fig. 3.2, and see Appendix A4, table A4.3). PC2 shows clearly the Bactrianus is different from all other Eurasian species, whereas skull morphology variation in *persicus* spans the distance between the Bactrianus mean and the more commensal Eurasian groups (fig 3.2).

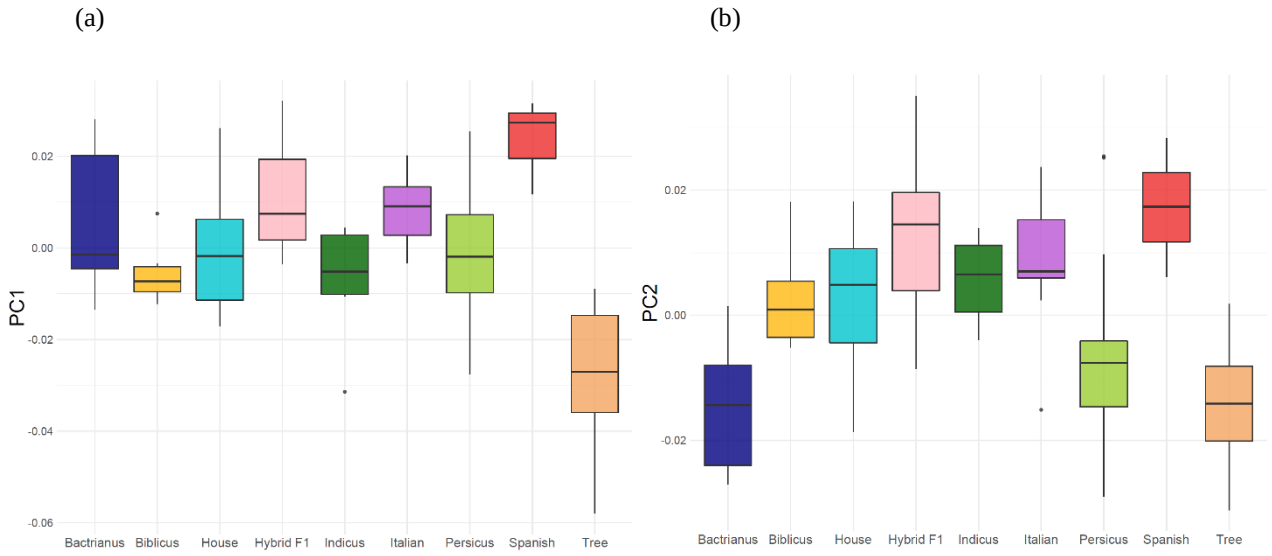

Figure 3.2. Boxplots of PC scores per group, for PC1 (a) and PC2 (b). Black line within each boxplot represents the sample median. Lower and upper limits of each box represent the 25 and 75% quartiles, respectively. Whiskers represent the minimum and maximum values, excluding outliers.

The predicted extreme shape changes along axes depicted by wireframes show that individuals with low PC1 values (which lie on the left side of the morphospace, namely tree sparrows) present on the lateral view: a more elongated vault along the anterior-posterior axis, a slightly higher frontal area, narrower nostril, lower insertion point of the jugal bone (which suggests a deeper beak) and a quadrate closer to the anterior than the posterior part of the braincase. On the dorsal view, tree sparrows show a narrower lachrymal and narrower and a beak pointed downwards. On the contrary, individuals with high PC1 values (mainly Spanish sparrows) show a deeper vault, lower frontal area, wider nostril, more elongated beak, although not longer (lateral view) and narrower lachrymal and beak (dorsal view). Essentially, PC1 accounts for major changes in the braincase, and the remaining shape variation (beak and palate) is minimal despite the exaggeration of the wireframes (Fig. 3.1b).

For PC2, beak differences are the clearest shape variation among groups (Fig 3.1c). There is a gradient between tree and Bactrianus sparrows (low PC2 values, blue wireframe) towards Italian and Spanish (high PC2 values, red wireframe). For high values of PC2 (red wireframe, lateral view) the craniofacial hinge is more elevated with respect to the rest of the cranium, whereas this point is much lower for low values of PC2. Interestingly, the beak shape around the nostril area of the blue wireframe creates a plateau, and the slope from this point to the tip of the beak is much more dramatic than in the high values of PC1. This makes their beak shorter and also more downwards pointed. This means that groups closer to Spanish and Italian sparrows in the morphospace have elongated and flattened beaks with respect to tree and Bactrianus sparrows.

3.1.1. Beak size

Centroid size of the whole skull was calculated out of 20 landmarks during Procrustes superimposition and was defined as skull size. There are obvious skull size differences ($F_{8, 77}$ = 41.18, $p < 0.001$, figure 3.3a, see tables and pairwise differences in Appendix A5, tables A5.1 and A5.2) between tree and Bactrianus sparrows and the rest; with these two being the smallest in the data set. We also found significant size differences between *persicus* and some of the larger subspecies (i.e., *biblicus*, Spanish).

Beak centroid size and the centroid size of the rest of the skull (i.e., vault, excluding beak landmarks) were studied separately, as well as the correlation between them.

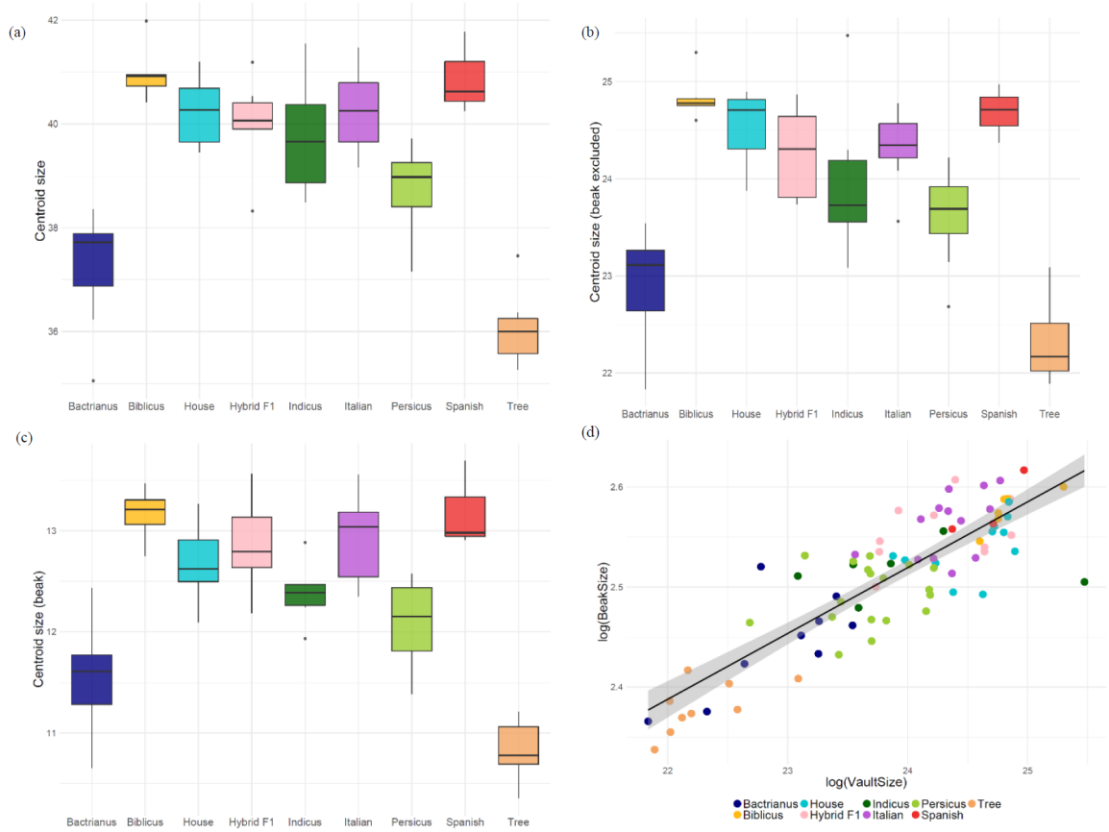

Figure 3.3. (a) Boxplot of skull centroid size for each group, out of 20 landmarks; (b) Boxplot of skull (excluding beak) centroid size (i.e.: vault) out of 12 landmarks; (c) Boxplot of beak centroid size out of 8 landmarks; Black line within each boxplot represents the sample median. Lower and upper limits of each box represent the 25 and 75% quartiles, respectively. Whiskers represent the minimum and maximum values, excluding outliers. (d) Linear regression between vault centroid size and beak size, both log transformed. Grey shading indicates standard error.

We found practically the same pattern in beak centroid size and skull (excluding beak) centroid size, with evident significant differences among species (beak: $F_{8, 77} = 35.27$, $p < 0.001$, figure 3.3.b; rest: $F_{8, 77} = 31.38$, $p < 0.001$, figure 3.3.c, and Appendix A5, tables A5.3 – A5.6) and a very significant correlation between both measures of centroid size ($t = 14.66$, $p < 0.001$, adj. $R^2 = 0.715$ and Appendix A5, table A5.7), indicating beak size scales with skull size.

3.1.2. Allometry

To test for allometry, we compared two nested models to explain Procrustes shape variation, using the geomorph function *procD.allometry()*.

The first model only included size as a dependent variable; the second included both size and a grouping factor (species or subspecies). An ANOVA test was used to compare these models (table 3.3). Thus the test indicates whether allometric relationships differ among groups.

After several model comparisons, the best model to explain shape variation (on Prucrustes data) was explained by size and species. Both variables have significant effects on shape although the correlation is not remarkably strong (R^2 for size ≈ 9%, R^2 for species ≈ 16.5%).

Table 3.3. ANOVA effect sizes and P-values based on empirical F distributions. ANOVA Type I (sequential) sums of squares and cross-products. Randomized residual permutation procedure used with 1000 permutations. Signif. codes: 0 '***' 0.001 '**' 0.01 '*' 0.05 '.' 0.1 ' ' 1.

	Df	SS	MS	Rsq	F	Z	Pr(>Z)
log(size)	1	0.013598	0.0135978	0.08970	9.1442	6.0431	0.001 **
species	8	0.024977	0.0031221	0.16477	2.0995	6.4045	0.001 **
residuals	76	0.113015	0.0014870	0.74553			
total	85	0.151590					

procD.allometry() also includes a Homogeneity of Slopes Test (HOS Test, table 3.4). The fact that differences in the slopes of allometric trajectories are not significant means that we can consider potential allometric issues across the whole data set at once, which additionally facilitates analyses and interpretation. The null hypothesis of parallel slopes was supported, based on a significance criterion of alpha = 0.05 (fig. 3.4).

Table 3.4. Homogeneity of Slopes Test

	Res Df	RSS	SS	MS	Rsq	F	Z	Pr (>F)
Common allometry	76	0.113						
Group allometries	68	0.105	0.007999	0.000999	0.052762	0.6474	-0.84916	0.802
Total	85	0.152						

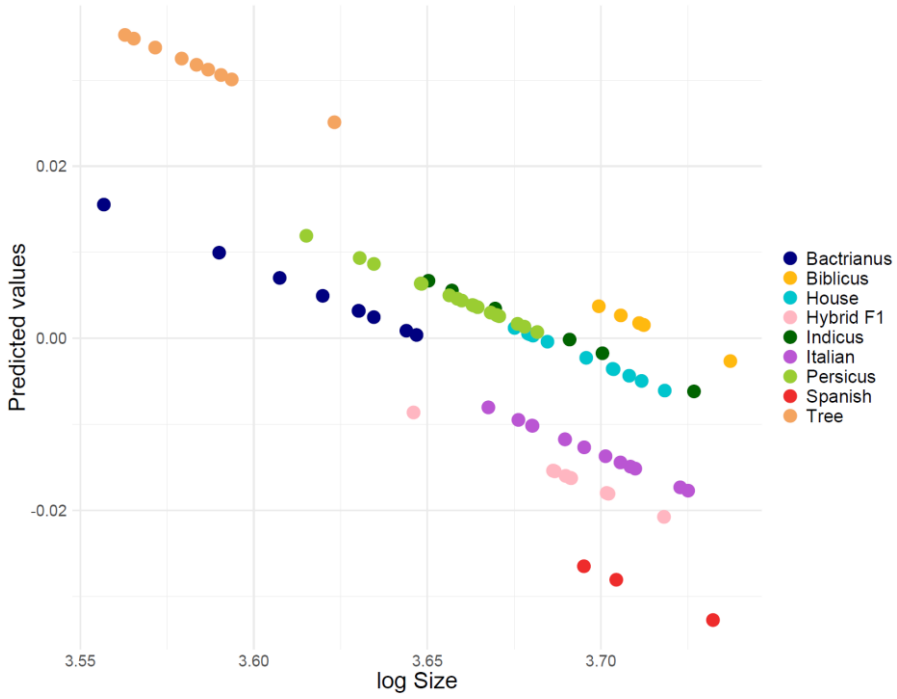

Figure 3.4. Y axis represents the predicted values from the regression of shape on size, and plots the first component of these versus log size, showing allometric trajectories. The slopes of these trajectories are practically parallel, showing that there is homogeneity of slopes and groups can be pooled together to deal with allometry issues.

3.2. Biting mechanical advantage

Biting mechanical advantage (MA) was calculated for a limited subset of House, Hybrid F1, Italian and Spanish sparrows (see methods). Data was distributed normally, but it was necessary to take special caution since sample size was small and not homogeneous among groups. Additionally, the density plot was left-skewed (see Appendix A6); as a result non-parametric tests were used. Although Kruskal-Wallis test does not present significant differences between species (Kruskal-Wallis chi-squared = 3.0206, d.f. = 3, p-value = 0.3885), there is a noticeable trend in the data. Italian individuals seem to have a larger mean and much larger variance. Despite this, results from Levene's tests for homogeneity of variance indicate that there are no significant differences in variance (center = median: $F_{3, 22} = 1.0177$, p-value = 0.4038; center = mean, $F_{3, 22} = 2.2518$, p-value = 0.1107; Fig. 3.6).

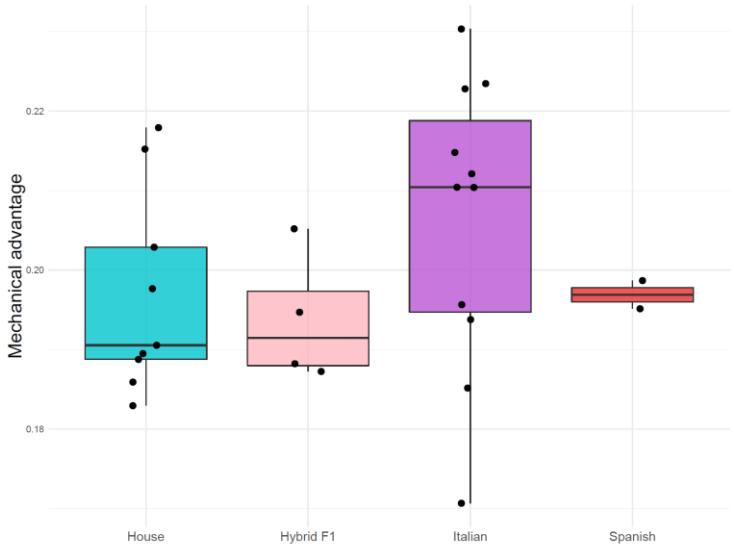

Figure 3.6. Boxplot of biting mechanical advantage for four groups. Each black dot represents one individual. Black line within each boxplot represents the sample median. Lower and upper limits of each box represent the 25 and 75% quartiles, respectively. Whiskers represent the minimum and maximum values, excluding outliers.

3.3. Relative brain size

Tarsus length was used as a proxy of body size in order to calculate relative endocranial volume for each skull and hence, relative brain size. The relationship between both log-transformed tarsus length and endocranial volume was calculated (table 3.5, fig. 3.5), and was both positive and significant ($p < 0.001$). Tarsus length explained around 21.1% of brain size.

Table 3.5. Coefficients of the linear regression between tarsus length and brain size. Residual standard error: 0.06105 on 72 degrees of freedom. Multiple R-squared: 0.2221, Adjusted R-squared: **0.2113**. Signif. codes: 0 '***' 0.001 '**' 0.01 '*' 0.05 '.' 0.1 ' ' 1

	Estimate	Std. error	t value	Pr(<|t|)
(Intercept)	0.18959	0.13436	1.411	0.163
tarsus	0.03214	0.00709	4.534	2.26×10^{-5} ***

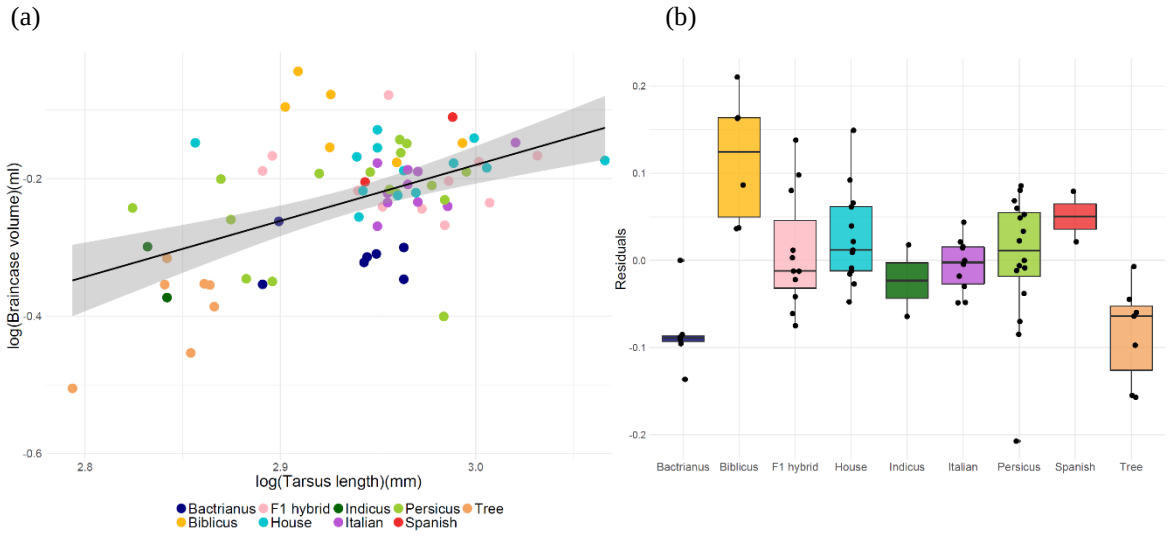

Figure 3.5. (a) Linear regression between braincase volume and tarsus length. Grey shading represents the standard error. (b) Boxplot of the residuals of the relationship shown in (a). Each black dot represents one individual. Black line within each boxplot represents the sample median. Lower and upper limits of each box represent the 25 and 75% quartiles, respectively. Whiskers represent the minimum and maximum values, excluding outliers.

We therefore performed ANOVA on the residuals of this relationship, showing significant differences between groups independent of body size ($p < 0.001$, fig. 3.5b, table 3.6, pairwise t-test can be found in the Appendix, A7).

Table 3.6. ANOVA test on the residuals of the linear regression shown in fig. 3.5 and table 3.5. Signif. codes: 0 '***' 0.001 '**' 0.01 '*' 0.05 '.' 0.1 ' ' 1

	Df	**Sum Sq**	**Mean Sq**	**F value**	**Pr(>F)**
Sp	8	0.1950	0.03427	6.695	2.31×10^{-6} ***
Residuals	65	0.2366	0.00364		

Significant pairwise differences (fig. 3.5b and Appendix A7) were found between Bactrianus and: Biblicus, F1 Hybrid and House, and also between Biblicus and: F1 Hybrid, House, Italian and Persicus. Tree sparrow relative brain size appeared to be significantly different from Biblicus and House.

3.4. Genome scans

We used linear models on Tajima's D and nucleotide diversity values with population grouping and gene status (i.e., candidate or null) as independent variables (with interaction terms included). A linear model with pairwise F_{ST} between Bactrianus and all other groups was also conducted in order to show differences between candidate and null genes.

We found a significant effect of both gene status (i.e., candidate and null) and population on values of Tajima's D (see model and pairwise differences in Appendix, A8) but no significant interaction (fig. 3.6a, $F_{7, 679} = 14.49$, $p < 0.0001$, $adjR^2 = 0.121$, when the interaction was dropped from the model). This means that at least some of the chosen 50 candidate genes might be under selection in certain populations, since the mean Tajima's D for candidate genes is lower than for null genes. Tajima's D was lowest in Bactrianus and Spanish sparrows (mean±SD -0.878 ± 0.578; -0.767 ± 0.646, respectively, for candidate genes only), and highest in house sparrow populations (-0.295 ± 0.676).

Regarding nucleotide diversity (fig. 3.6b), we found no gene status or population effect, nor a significant interaction ($F_{13,679} = 0.294$, $p = 0.993$, $adjR^2 = -0.013$). Although there is a general trend of candidate genes showing lower nucleotide diversity than null genes, there is no obvious difference among populations (fig. 3.6b).

When examining pairwise F_{ST} between Bactrianus and the rest, (fig, 3.7), we did not find significant effect of gene status ($F_{5,594} = 69.52$, $p < 0.0001$, $adjR^2 = 0.364$). Pairwise F_{ST} between Bactrianus and the rest of Iranian house sparrows (*biblicus*, *indicus* and *persicus*) is near zero, showing almost no differentiation among Iranian populations for both candidate and null genes. However, there are substantial differences in pairwise F_{ST} between Bactrianus and European house, Italian, and Spanish sparrows, showing an increasing gradient of differentiation in this order.

Some Tajima's D outliers for the 95th percentile of the 50 candidate genes seemed to overlap in several populations. We subsequently chose five major candidate loci, based on their importance in skull and beak morphology in the literature in order to study where their values lie in this framework. For instance, *TFGB2* (upregulation in *TGFB2r* results in deeper and larger beaks in finches) showed the highest Tajima's D value (0.954) in house sparrows, whereas it was very low in the rest of the groups (sometimes appearing as an outlier, like in Bactrianus (-2.38) and Spanish (-2.22) populations). On the contrary, *Col11a1* (which regulates craniofacial and skull development) appears to exhibit an extremely low value and is an outlier in European house populations (-1.46). However the same gene has much higher values in Iranian house and Spanish (*biblicus* = -0.335, *indicus* = -0.165, *persicus* = -0.346, Spanish = 0.0950). Another gene that shows differences among populations is FZD1 (its upregulation produces wider beaks in finches), which has a low Tajima's D for all groups (≈ - 1.73 on average) except for *persicus* (0.434), where it is positive.

Negative Tajima's D outliers do not seem to correlate with nucleotide diversity for the five focal craniofacial candidate loci. In terms of nucleotide diversity, they show similar pattern among groups: *BMP4, FDZ1* and *ALX1* nucleotide diversity is generally lower than the median of the 50 candidates. *TGFB2* and *Col11a1* tend to present nucleotide diversity values larger or similar to the mean across each of the species/groups, especially *TGFB2* nucleotide diversity in house ($\pi = 0.0110$) and Italian sparrows ($\pi = 0.00698$).

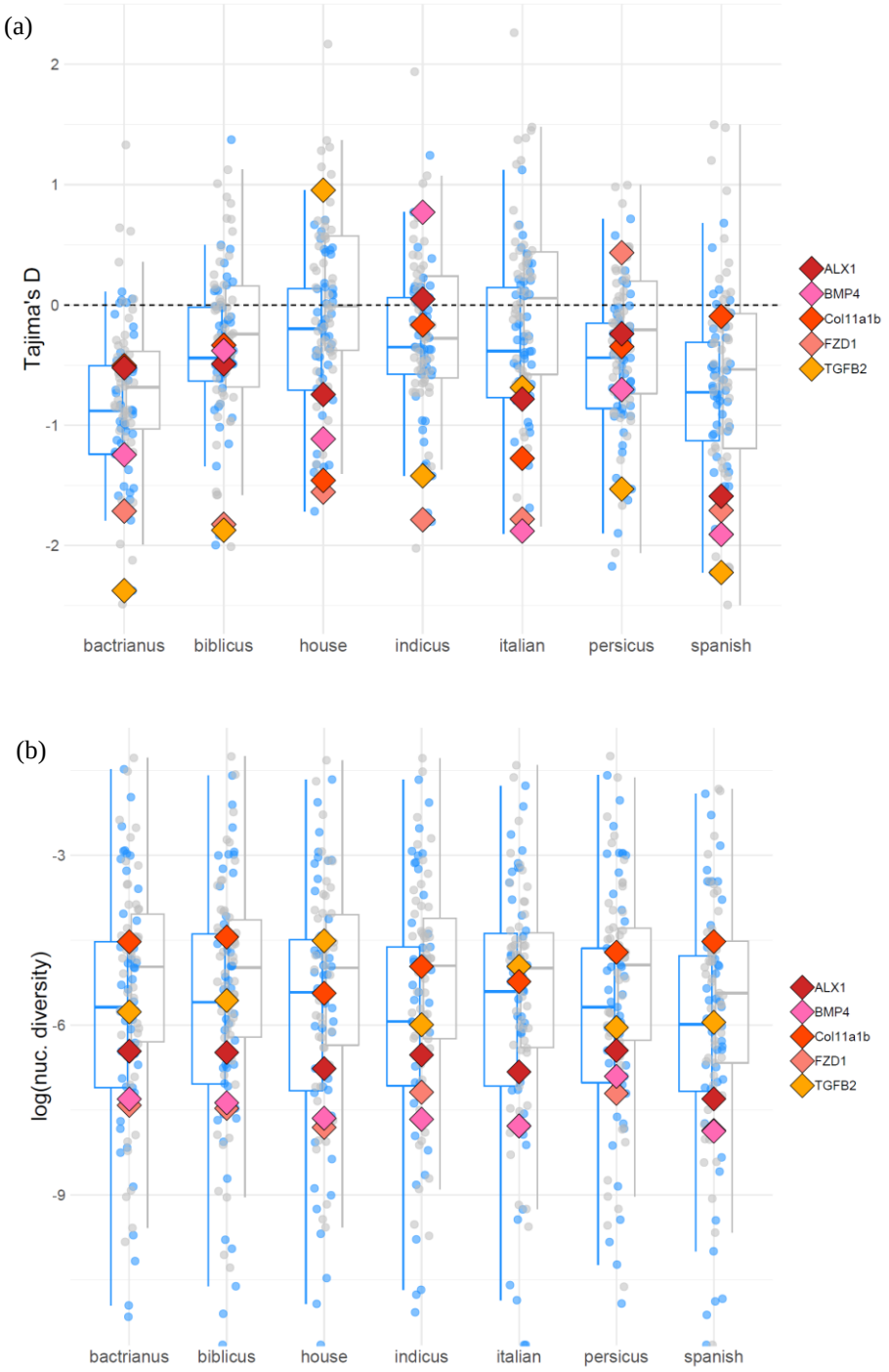

Figure 3.6. Blue boxplots represent Tajima's D (a) and nucleotide diversity (b) values for each population for the candidate genes. Grey boxplots represent Tajima's D (a) and nucleotide diversity (b) values for each population for the null genes. Thick lines within each boxplot represent the sample median. Lower and upper limits of each box represent the 25 and 75% quartiles, respectively. Whiskers represent the minimum and maximum values, excluding outliers. Blue and grey points over the boxplots represent Tajima's D (a) and nucleotide diversity (b) values for each candidate and null gene respectively. The large, coloured diamonds represent five key genes know to play a role in the development of beak and skull morphology (see legend for further details).

Pairwise F_{ST} between Bactrianus and the rest of the groups in our focal five genes also show an interesting pattern (fig. 3.7). *TGFB2* presents an extremely high value for a value like F_{ST} in Spanish (0.849) and Italian (0.691), and is still somewhat large in house sparrows (0.312). *ALX1* and *BMP4* F_{ST} are also fairly large in these populations compared to the Iranian commensals (*ALX1* F_{ST} Bac- Sp = 0.341, -It = 0.198, -H = 0.191; *BMP4* F_{ST}Bac – Sp = 0.253, - It = 0.195, -H = 0.172). Interestingly, *Col11a1* presents large F_{ST} in house and Italian Sparrows (0.213 and 0.202 respectively), but values for this gene are relatively lower in all other comparisons (including in Spanish sparrows, 0.102). *FZD1* values are low in each pairwise comparison, but they are not outliers.

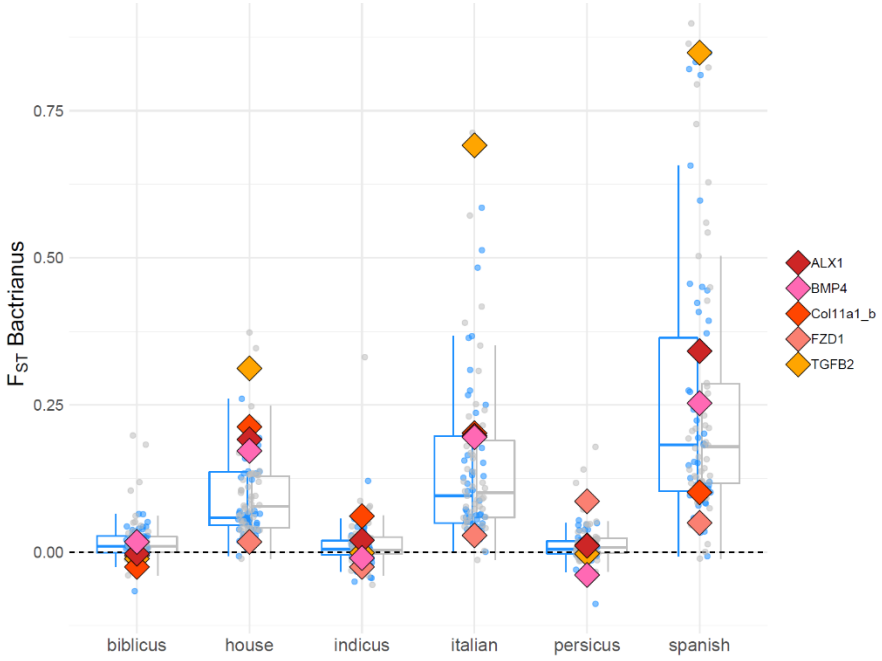

Figure 3.7. Blue boxplots represent F_{ST} values between Bactrianus and each population for the candidate genes, and grey boxplots for the null genes. Thick lines within each boxplot represent the sample median. Lower and upper limits of each box represent the 25 and 75% quartiles, respectively. Whiskers represent the minimum and maximum values, excluding outliers. Blue and grey points over the boxplots represent F_{ST} for each candidate and null gene respectively. The different big black shapes represent five important genes for beak and skull morphology: The large, coloured diamonds represent five key genes know to play a role in the development of beak and skull morphology (see legend for further details).

4. Discussion

4.1. Skull morphology and feeding performance

We detected differences in skull morphology between groups, which may explain a phenotypic distinction between non-commensal (namely the Bactrianus and tree sparrow) and commensal ecologies (the remaining groups – i.e. the house sparrow in Europe and Iran).

The major difference between the tree sparrow and all Eurasian species is variation in the neurocranium, and the main axis of variation among the Eurasian species is driven by differences in the splachnocranium, especially in the upper jaw. The splachnocranium includes the upper jaw or maxilla, lower jaw or mandible, jugal bars, palate and quadrates. This region connects with the neurocranium (i.e.: the braincase) only by synovial joints of the quadrate and palate, and by a flattered elastic bony zone (the craniofacial hinge or nasal-frontal hinge) of the upper jaw (Hall, 1993) (Fig. 4.1).

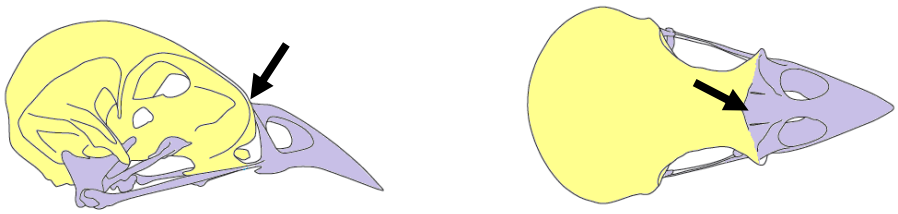

Figure 4.1. Lateral and dorsal view of a sparrow skull. Yellow shading represents the neurocranium and purple represents the splachnocranium. Arrows indicate the position of the craniofacial hinge.

Commensals appear to have a longer and flatter upper beak, higher orbital process, wider ectethmoid-lachrymal complex, narrower interorbital area and wider nostril, compared to non-commensals. Despite their geographical proximity, Bactrianus sparrows are clearly separated from the commensal subspecies in Iran as well as the house, Italian and Spanish sparrows in Europe. In short, Bactrianus is more similar to the tree sparrow in splachnocranium structure.

Our results are consistent with previous work that examined variation in skull morphology on *Passer* sparrows from Iran (Riyahi et al., 2013). Skulls of commensal house sparrows from

Norway and Spain group together with the Iranian commensals: *biblicus*, *indicus* and *persicus* (although *persicus* individuals appear more diffuse in the morphospace). The fact that Bactrianus and *persicus* are more similar -morphologically speaking- to each other has also been suggested by Riyahi and colleagues, since they also overlap greatly in the morphospace in their study. However, these authors pinpointed observable differences when exploring the dorsal view of both Bactrianus and *persicus* skulls, with *persicus* generally appearing more robust (where robustness is defined as a personal observation of bone density or thickness). In the present PCA, *persicus* overlaps with multiple groups, both in PC1 and PC2. Most *persicus* individuals occupy the same space as Bactrianus, whereas the rest overlap with house, *biblicus* and *indicus*. The ecology of *persicus* is associated with anthropogenic environments, and it apparently does not interbreed with Bactrianus, at least in view of observational data in the literature (Summers-Smith, 1988; Saetre et al., 2012, Riyahi et al., 2013), although their home range overlaps. However, one potential explanation is that they might have interbred in the past, and thus show partially shared phenotype in skull and centroid size. Despite Bactrianus should have whiter cheeks and underparts (Summers-Smith, 1988), it is also possible that some *persicus* might have been mis-identified as Bactrianus (G-P. Sætre, personal observation), or that their phenotypes have converged due to habitat overlap.

On the other hand, the remaining commensal Iranian groups (*biblicus*, *indicus* and *persicus*) overlap with one another, occupying a considerable area in the morphospace but with the Bactrianus further away. This is also congruent with Riyahi's shape analysis based on outlines (Riyahi et al., 2013) and an apparent lack of population structure among these groups when studying mtDNA and cDNA (Sætre et al., 2012).

This intraspecific variation between Iranian commensals is a factor that should be taken in account. For instance, a recent study on *biblicus* and *indicus* sparrows in Israel, showed significant differences in size and coloration along a latitudinal gradient, in accordance with Bergmann's and Glogger's biogeographic rules. They show that these traits appear to be quite plastic, since genetic differentiation was lower than phenotypic variation (Cohen & Dor, 2018). Due to low sample size and unavailable sex data for some groups, we could not test whether this intraspecific variance in skull morphology is a consequence of sexual dimorphism, although differences in several morphological traits and in their heritability between sexes have been addressed in house sparrows of northern Norway (Jensen et al., 2003).

Consequently, skull morphology does not support the distinction between the Iranian commensal subspecies. However, they appear to be distinguishable in terms of plumage coloration and size, according to Summers-Smith observations (1988) and it can be argued that this phenotypic variation might be purely biogeographical. Furthermore, genomic data reflects a clear division between Bactrianus and house (Ravinet et al., 2018), but it remains unclear whether this is the case of the other Iranian subspecies, and a deeper investigation into their relationship is necessary.

Thus, the wild Bactrianus sparrow is more similar to the tree sparrow in splachnocranium shape (specifically in the beak) and size than in neurocranium structure. This is interesting since both species are assumed to exhibit similar ecologies in Europe and the Near East (i.e. wild or non-commensal, although tree sparrows have shown ability to adapt to highly urbanized environments in Eastern Asia, - e.g. Maeda, 1998, Chen & Wang, 2017). Hence, changes in feeding apparatus between commensals and non-commensals show that commensal sparrows have likely undergone an adaptation to the consumption of larger and harder seeds from cultivated crops.

Beaks have historically been subject of the study of adaptation to novel environments, associated with different feeding strategies, and sometimes forming the basis of rapid and impressive adaptive radiations. Probably one of the most iconic examples of adaptation of beak morphology to food availability is that of the Darwin's finches (Grant & Grant, 1996). This system has been extensively studied, and several of the genes which play a role in the different dimensions of the beak during development have been identified (Mallarino et al., 2011). Such examples and the evolutionary history of the sparrow system suggest that a relationship between beak shape and/or size and feeding preference is present and can be demonstrated, at least at a population level (e.g., Runemark et al., 2018 on Italian sparrows, where they show that changes in beak shape were explained by variation in carbon isotopic ratios). Additionally, among the different modules of the bird skull, the beak appears to be one of the most evolvable, with a higher evolutionary rate than other modules, such as the basisphenoid, the pterygoid or the quadrate (Felice & Goswami, 2018). Despite a well-developed understanding of beak evolution in systems such as Darwin's finches, there are still limits, suggesting that the picture might be more complex than expected (i.e., there are many genes acting upon different dimensions beak

morphology and size, and their relationship appears to be extremely intricate (e.g., Mallarino et al., 2011, Lamichhaney et al., 2015, Lawson & Petren, 2017).

However, how are changes in skull morphology obvious adaptations to larger and harder seeds in our system? One of our major findings is that commensal sparrows have longer, wider and flatter beaks than non-commensals, which is likely an important adaptation facilitating feeding on larger and harder seeds. These changes in seeds arose independently in multiple settlements of hunter-gatherer societies across the world. One of them is our area of interest, the Near East, where mainly barely, wheat and several legumes species were first cultivated between 13K and 10Kya (Purugganan & Fuller, 2009). It has been studied that enlargement in these crop species actually occurred during the process of plant cultivation for human consumption (Kluyver et al., 2017, Fuller & Allaby, 2018).

Beak and skull morphology and seed husking and cracking have been previously studied in other bird species, demonstrating a trend for seed selection depending on bill and skull shape and size. For instance, beak depth, width and shape and head width were significant predictors of bite force in Darwin's finches, where head width played an important role in jaw biomechanics when eating harder seeds (Herrel, Podos, Huber & Hendry, 2005). In addition, it appears to be that deep and wide beaks in ground finches would also limit high peaks of mechanical stress and subsequent risk of beak failure, which is key when an increase in biting force is needed (Soons et al., 2010).

In sum, we consider that changes in skull morphology –and specially beak shape- are essential to differentiate these sparrow populations and study their relationship with feeding performance. Although the study of biomechanics on these species is not one of the main goals in this project, it is important to examine the kinesis of the whole cranium in order to understand structure, function and evolution of the avian head (Bock, 1964), as well as non-bony structures such as muscles and ligaments.

For instance, in this case beak shape in commensals (i.e., longer, wider and flatter) appears to covary with a higher craniofacial hinge, which is a bending region at the junction of the nasal and frontal bones that makes the upper jaw act as a unit. This tendency towards a more structurally integrated splachno- and neurocranium and the increased robustness in this area

might be related with a less flexible craniofacial hinge in commensals, which would allow them to develop a stronger and more precise bite force. This is supported by Bock's studies (1964) (based on both tests in passerines and available literature) where he argues that the extent of freedom of the upper jaw depends considerably on the structure of the hinge and its relatively bony nature.

Other interesting changes that might be related to feeding performance (or at least seem to covary with traits related to feeding performance) are the insertions of the jugal bar with the upper beak, the quadrate with the braincase, the orbital process, the ectethmoid-lachrymal process and the widths of the interorbital area and the nostril.

It was not possible to place a landmark in the insertion of the jugal with the quadrate (or any other point on this bone) because for most samples this bone was either lost or deattached from the rest of the skull. This is unfortunate since the quadrate is a key structure that connects the most important units of the skull: braincase, upper jaw, palate and lower jaw. Consequently, it plays an important role in kinetics, because it articulates dorsally with the braincase, ventrally with the lower jaw, ventro-laterally with the quadratojugal and anteriorly with the pterygoid (Zusi, 1993). In addition, the prominent orbital process of the quadrate is utilised for muscle attachment. Although our results do not reveal clear differences among the species, we hope future skull collections attempt to include this structure.

The insertion of the quadrate with the braincase was studied and appears to be lower in commensals than in non-commensals. A quadrate that originates closer to the ventral margin of the skull will make more space between the upper and the lower jaw when the mandible is open, which will probably be useful if these individuals are eating larger seeds. Moreover, quadrates in commensals seem to be more robust (based on personal observations of bone density). The pterygoid and palatine also connect upper and lower jaw and their structure needs a more detailed understanding to address differences in biting performance.

We also see differences in the lachrymal and the orbital area, which is congruent with Riyahi's et al. work (2013). The ectethmoid-lachrymal complex appears to be more prominent in commensals, and this structure is associated with limiting the amount of the kinetic movement in the upper jaw through ligaments (Bock, 1964). In any case, there are other structures responsible for jaw movements, such as differences in other articulations, muscles, ligaments and flexible bony hinges. Examining fresh tissue in more detail may shed light in our

understanding of shape and feeding performance in this system (e.g. Van der Meij & Bout, 2004; Soons et al., 2010), as well as conducting digital muscle reconstructions (e.g. Lautenschlager, 2013; Lautenschlager et al., 2014).

Furthermore, the braincase protects the brain, eyes and ears from the forces and impacts resulting from jaw action (Bock, 1964), and thus, changes in beak shape to adapt to bigger and harder seeds may also have an increase in the overall robustness of the skull (in terms of bone density or thickness). This increased robustness and body size in commensal sparrows might also be due to their sedentary habits, since they do not perform frequent and long flights associated with migration, unlike tree and Bactrianus sparrows (Riyahi et al., 2013). However, we are basing our understanding of robustness on how prominent these structures are (from shape analysis), personal observations and literature. Calculating bone density or bone thickness in certain areas of the skull would provide more formal evidence and we would like to perform this analysis in the future.

Interestingly, we see that Spanish sparrows are placed at high values of both PC1 and PC2. They greatly overlap with the Italian sparrow, producing a gradient between Spanish and house –its two parent species, which is particularly noticeable when we look at the mean shape for each group. This is consistent with the phenotypic and genomic moisaicism present in Italian sparrows (Elgvin et al., 2017), which likely also applies to skull morphology. Spanish, Italian and F1 hybrids appear to be more compact in the morphospace (towards the upper right area of the PCA) than the Iranian sparrows and the European house, which are more spread out, especially in the case of *persicus*. This suggests that skull variation in house sparrow subspecies (from Iran, Oslo and Spain) is larger than in the studied Italian and Spanish populations. This might occur because the house sparrow distribution is larger and faces a wider range of environmental variation, meaning that it is more likely that they present more variability among populations. The same rationale could be applied to Spanish sparrows, but unfortunately, only three samples from one population could be included in this study. Skulls from a wider range of Spanish and Italian sparrow populations will be necessary for future work.

In any case, Spanish sparrows are not much associated with anthropogenic environments, prefer to occupy more mesic habitats, and they are in general more specialists compared to House and Italians. A simple naïve hypothesis is that the Spanish sparrow would tend to lie closer to

Bactrianus and tree sparrows, since their food preferences might be similar, but the PCA places of these groups at opposite ends of the major axes of variation. This could result from low sample size, plasticity/biogeographical reasons, unstudied allometric constraints (Spanish have a larger centroid size, similar to Italian and House, and present the same beak shape as these species). Another possibility is that beak shape does actually not play a major role in feeding performance in Spanish sparrows (i.e., there are other phenotypic traits that can explain these ecological differences (such as biomechanical or behavioural). Additionally, Spanish introgression into the house sparrow (Ravinet et al., 2018) might have made the morphology of the house more Spanish-like, and that this, in conjunction with other traits, such as starch digestion ability, is what has made the house a successful commensal.

Whereas we postulate that a change in food availability and habits due to the spread of agriculture and urbanization has affected the morphology of the sparrow skull, other studies suggest alternative explanations. One of the most recent and integrative approaches to link beak shape, size, feeding performance and feeding strategy suggested that the relationship between beak shape and feeding ecology is not so straightforward as it has historically been thought, at least at a macroevolutionary level (Navalón et al., 2019). This might occur because selective pressures that act upon the beak are involved in other functions besides feeding, such as preening, vocal modulation, nest construction or thermoregulation among others, and also developmental and/or allometric constraints. Additionally, similar hypotheses have been tested on the whole cranial structure using high dimensional geometric morphometrics, obtaining the same conclusions (Felice, Tobias, Pigot & Goswami, 2019). Although studies on two textbook examples of island adaptive radiation (Darwin's finches and Hawaiian honeycreepers) have linked cranial morphology with food type, they also recognize that some birds that overlap in the morphospace present different diets (Tokita, Yano, James & Abzhanov, 2017). This mismatch between shape and feeding ecology has been shown in birds of prey (Bright, Marugán-Lobón, Cobb & Rayfield, 2016), arguing that allometry and phylogeny can act to constrain beak shape diversification.

Despite uncertainty whether the shift from wild-type small seeds to larger seeds from crops has acted upon skull morphology in terms of feeding performance, we found evidence suggesting that Bactrianus differs significantly from the others. Furthermore, macroevolutionary trends do not necessarily explain these differences at the species or genus level. The evidence is consistent

with the hypothesis that these changes in skull morphology have likely facilitated the switch from wilder habitats to rural and urban environments or the adaptation to human niches.

As we have mentioned before, biomechanics can reveal multiple aspects of feeding performance. Changes in skull shape and their relation with feeding strategy might fall in being be purely descriptive and speculative, and should be tested in a more practical way (this has been previously done in Darwin's finches; De León et al., 2011). We believe that studying feeding performance through biting mechanical advantage can link (at least partially) shape and feeding strategy.

Although we did not find any significant difference in mean or variance among groups in biting MA calculations, Italian sparrows appear to present a more forceful bite on average than the rest (including hybrid F1 - i.e. artificially generated Spanish x house hybrids), and their variance is also larger. Biting MA is a measure of efficiency, so this would mean bite force in house, hybrid F1 and Spanish sparrows is lower, but faster. It has been previously shown that Italian sparrows present more variability not only in beak shape but also in dietary preferences (from stable isotopes analyses) between and within populations, when compared in allopatry and sympatry (with Spanish sparrows), mainland and island and between different islands (Eroukhmanoff, Hermansen, Bailey, Sæther, & Sætre, 2013; Piñeiro, 2015; Sætre et al. 2017, Runemark et al., 2018), which is congruent with a larger variance in biting MA.

We expected to find higher biting MA in house and Italians and lower in Spanish, because house and Italian sparrows would need a more forceful bite when eating harder and more encapsulated seeds from crops. Although we found no significant differences in biting MA, these results do not contradict this hypothesis, since our PCA showed that changes in beak shape in this subset of species were minimal (although Navalón et al. (2019) found little correspondence between beak shape and biting MA in their macroevolutionary study).

In addition, there might be other factors that can bias these results. For example, our samples do not include the rhamphotheca, which is a keratine thickening that covers the beak and has been shown to play a role in stress dissipation of bite force in finches (Soons et al., 2012). Another possibility is that different groups might follow different strategies in terms of seed crushing: we have only calculated biting MA at the tip of the beak, but results might change if

we included the more caudal areas of the beak. Seed handling might differ between populations, meaning that if husking is efficient, biting force may be less relevant, as it has been studied in finches (Van der Meij & Bout, 2006). In any case, more samples from different populations need to be included in order to clarify this trend, combined with actual measures of bite force, to actually study whether they show correlation with biting MA calculations.

A comment on allometry correction, beak and skull size

Shape was significantly affected by size and the grouping variable (species or subspecies), but their contribution was not substantial. The grouping variable explains approximately a 16.5% of the shape variance, and size (as log-centroid size) only 9%, and their interaction was not significant.

This has several implications: (1) the residuals explain three quarters of the shape variance, meaning that intraspecific variation is considerable and that might be other predictors that contribute to shape besides individual variation, such as sex (in some groups sex was underrepresented and there was a considerable amount of non-available data), population (within species and subspecies) and environmental variables; (2) our grouping variable (species and subspecies) was not able to completely explain shape variance in skull morphology, indicating that different phenotypes are present in multiple species or subspecies; and (3), the effect of size explaining shape is minimal. Briefly, shape only marginally covaries with size. This means that, the shape of a certain individual is not constrained by its centroid size, or that, the fact that a particular individual has a larger skull, does not mean that it will present a certain shape.

To study allometric effects we have followed the Gould-Moissman school approach, by which size and shape are conceptually and mathematically separated, and this is the reason why we have used the residuals of the regression Procrustes data ~ log(size) to study shape variation (although allometry hardly affected the PCA, see Appendix A4, fig. A4.2). Allometry corrections based on the Gould-Moissman are widely used in similar studies (e.g. Tokita et al., 2017) rather than Huxley-Jolicoeur approaches. Additionally, if the studied shapes and sizes are fairly similar and allometry is weak, differences of allometry-corrected morphospaces between both schools would be fairly subtle (Klingenberg, 2016).

However, the study of size itself can also shed light on adaptive evolutionary processes. For instance, a study on birds of prey showed that size was the major predictor for feeding ecology, rather than beak shape (Bright et al., 2016), although size differences in this non-monophyletic group are dramatic. They also showed that beak shape was strongly correlated with neurocranium shape, with these two structures being very integrated. However, at a genus and species level, beak size appears to vary more independently as a response to selective pressures, even more than beak shape. This is presented in a 30-year study on Darwin's finches (Grant & Grant, 2002) where body and beak size traits were selected more frequently than changes in beak shape.

In the present study, the centroid size of the whole skull is much bigger in commensals than in Bactrianus and tree sparrows (consistent with Riyahi et al., 2013). However, the independent log centroid sizes of the braincase and the beak are strongly correlated (adj. $R^2 = 0.715$), meaning that beak size variance is considerably constrained by (at least) neurocranium size in *Passer* sparrows.

In sum, centroid size has little impact on skull morphology and allometry is subtle, although we have still attempted to correct for it. Beak centroid size correlates with skull centroid size (excluding beak), meaning that if beak size is being selected for eating larger and harder seeds, it is in concordance with the rest of the skull.

4.2. Relative brain size

Tarsus length explained 21% of the variation in brain size. This is a considerable percentage, but studying the remaining variation showed that both non-commensal species, Bactrianus and tree sparrows present a significantly smaller brain size. Unfortunately, sample sizes for this test were reduced and some groups such as *indicus* and Spanish were clearly underrepresented. In any case, the trend is evident, and we can confirm the large-brains hypothesis in this system. This theory, (also called 'cognitive buffer hypothesis', CBH, e.g., Allman, McLaughlin & Hakeem, 1993; Deaner, Isler, Burkart & Van Schaik, 2007; Sol, 2008) states that a relatively large brain would enhance cognitive abilities in fluctuating environments. Our results support

relatively recent works on a large range of bird species (Sayol et al., 2016), which were more likely to present relative bigger brains when exposed to unpredictable environmental variation, through phylogenetically-based comparative analyses.

However, Healy and Rowe (2006) recommend being cautious with regard to relative brain size studies and its dubious correlation with complex behavioural patterns. Correlating a certain behaviour to the enlargement of the brain -or a particular area of the brain-, which is supposed to perform different functions might be controversial. The theory of sedentary animals showing bigger brains is also questioned, because they need to face larger environmental variation, indicating that complex migratory patterns and food availability issues during the trip of migratory birds would also enhance high behavioural complexity, and hence, the development of relatively bigger brains (although increased brain weight should not be an issue during migration; this trade-off has been recently studied by Vincze (2016)). This review proposes other limitations such as the implementation of indirect measurements of relative brain size, the assumption that brain size does not change during the animal lifespan and the vague integration between brain size and life history traits in the literature.

We are aware that estimating relative brain size and correlating it with complex behaviours (in this case the capacity to face unpredictable environments, more specifically in terms of food availability) should be considered with caution. However, the relationship between brain size and innovation rate has been studied recently (e.g., Ducatez, Clavel & Lefebvre, 2015) and our results support this hypothesis on a well-known human commensal species: sparrow commensals are much more associated with highly variable anthropogenic environments and they do not migrate, in comparison with Bactrianus and tree sparrows.

In addition, an integrative study presented recently showed that innovation rate is linked to an investment in future rather than immediate reproduction, and that this is partially explained by relative brain size (Sol, Sayol, Ducatez & Lefebvre, 2016). The conjunction of innovation and life history traits is more likely to evolve in generalist and opportunistic species, which constantly face environmental change (Sayol et al., 2016; Sayol, Downing, Iwaniuk, Maspons & Sol, 2018). Anthropodependent species (Hulme-Beaman et al., 2016) such as house sparrows are supposed to encounter unpredictabilities in urban and rural environments. Urbanization itself has also been associated with relatively bigger brains (e.g., 22 families of passerines have shown bigger brains when living in urbanized niches than in rural areas, tested in 12 different

cities (Maklakov et al., 2011)). However, other studies on birds have not shown this correlation (Kark et al., 2007, only in Israel area).

We have measured endocranial volume as a proxy of brain size, but we have not tested whether the brain grows evenly in commensal species or whether certain regions of the brain tend to grow larger than others. It has been suggested that the forebrain appears to be larger when linked to feeding innovation in birds (Lefebvre, Whittle, Lascaris, & Finkelstein, 1997; Rosza et al., 1998, Lefebvre & Nicolakakis, 2000). Studying the differences in brain shape on our study species might reveal something similar, and testing this would be plausible without the actual brains, since CT scans provide us the possibility to explore the internal structure of the braincase. In any case, external neurocranium shape does not appear to correlate with brain size, since tree and Bactrianus sparrows present similar brain size and different cranium shapes.

4.3. Genome scans

The genomic architecture of beak and skull morphology comprises a complex scenario where many genes likely play a role in the formation of this trait, as has been shown in previous studies, mostly on Darwin's finches (Mallarino et al., 2011; Lamichhaney et al., 2015; Lawson & Petren, 2017). This is the reason why we chose 50 genes of potential interest in the development of craniofacial morphology in birds, as well as other genes of interest, such as *AMY2A* (linked to a shift to starch-based diets in humans and dogs during the Neolithic revolution (in humans, Perry et al., 2007; in dogs Axelsson et al., 2013)) and *PARL* (it shows increased expression during migration in brains of white-crowned sparrows, (Jones, Pfister-Genskow, Cirelli & Benca, 2008)). These two genes were previously shown to exhibit signatures of selection in commensal house sparrows (Ravinet et al., 2018). Therefore, we used these 50 candidate genes to test for a general trend for signatures of selection, although most of them were not outliers, or if they were, they did not overlap in populations with similar ecologies (in any case, a further investigation of those loci is needed). We further narrowed down our list to five genes that have been key for changes in beak and skull morphology in birds and examined them in more detail. These five genes were chosen because they showed

very low Tajima's D value and/or high F_{ST} and because of their functional importance in beak and skull morphology in the literature.

Tajima's D analyses show that on average, the 50 candidate genes are more likely to be under selection or linked to a selective sweep, compared to a set of randomly chosen coding genes, which have significantly higher Tajima's D values. However, candidate genes show that evidence of selection varies among populations. This might occur because different genes might be involved in similar morphological changes, or because different selective pressures acting on certain populations might be driving different morphological changes. Inferring the genomic architecture that underlies these kind of processes is a great challenge, also because of the large modularity of the different networks that act upon in different species, as it has been shown in previous studies of Darwin's finches and Caribbean bullfinches (Mallarino et al., 2012).

Despite the fact that candidate genes exhibit lower Tajima's D than the null genes their values per population appear to correlate. These changes among populations might give us some information about demographic changes. For instance, negative values of Tajima's D are generally related to population expansion (i.e., rare alleles are present at high frequencies), like in the case of Bactrianus and Spanish sparrows. Their Tajima's D is lower compared to the other species, potentially because these populations are still increasing in size, as a result of population contractions during the Pleistocene. The rest of populations appear to lie close to zero, suggesting that they probably are approaching demographic equilibrium.

Regarding Tajima's D values for the five focal genes, *TGFB2* represents good evidence of selection. It appears to be strongly selected for Iranian and Spanish sparrows but shows very high Tajima's D in house, and similarly a relatively high value in the Italian sparrow. Therefore, this gene appears to be highly variable among populations (both nucleotide diversity and pairwise F_{ST} against the Bactrianus support this). One potential explanation is that different alleles of *TFGB2* might be selected to favour particular morphological traits in the beak (the upregulation of the receptor of this gene (*TFGB2r*) is involved in longer and deeper beaks in finches) in different populations (Mallarino et al., 2011). This suggests a case of balancing selection. F_{ST} values for *TGFB2* are congruent with this hypothesis, showing extremely high values in Spanish and Italian sparrows. The fact that the house sparrow has arisen from a non-commensal ancestor (i.e., Bactrianus) and later introgressed with the Spanish (eventually giving rise to the Italian) (Ravinet et al., 2018) might have made this species polymorphic for divergent alleles, and this polymorphism might have been maintained by balancing selection (this type of

selection appears to maintain divergent alleles in the Italian sparrow too (Elgvin et al., 2017)). This has probably developed the emergence of changes in skull morphology in the house: an evolutionary novelty ideal for the adaptation to a shift in dietary preference and/or habits in anthropogenic environments.

Col11a1 also shows interesting values of Tajima's D, nucleotide diversity and F_{ST}. This gene has been previously associated with changes in craniofacial morphology in commensal house sparrows (Ravinet et al., 2018). Our results support these previous findings and show that there is evidence for selection for *Col11a1* in house and Italian populations due their low Tajima's D values compared to other, non-commensal populations. Additionally, this gene does not appear to be under selection in the Iranian populations either. This trend is also demonstrated by higher values of F_{ST} for this gene, although its impact is not as dramatic as *TGFB2*. Contrary to *TGFB2*, selection for *Col11a1* appears to have emerged in European house sparrows populations only and is also present in its hybrid (i.e., Italian sparrow). This means that selection on this gene likely occurred after the split from Bactrianus but prior to the hybridisation events leading to the Italian sparrow.

Regarding *FZD1*, it appears to be under selection in all species, but its F_{ST} is not especially high in any of them. One possibility is that this gene might be undergoing recurrent selective sweeps by purifying selection, but it is not divergent among populations. Alternatively, *FZD1* has potentially swept across species boundaries and spread by adaptive introgression, since all these populations have shown evidence of past introgression. Therefore, further work is necessary to see if this gene has potentially swept across species boundaries and spread by adaptive introgression, since it has a role in the *wnt* pathway, which can lead to the development of wider beaks (on sparrows, Lundregan et al., 2018).

BMP4 is clearly not a Tajima's D outlier, except in the case of Spanish sparrows. It is noticeable again that Tajima's D values for Italian and house are also low. Probably selection for this gene has arisen in the Spanish sparrow and the introgression with the house (and the subsequent rise of the Italian) might explain this trend. This is also congruent with the morphological data and this gradient we see between the Spanish and the house, since the upregulation of this gene accounts for deeper and wider beaks (on Darwin's finches, Abzhanov et al., 2004). This same pattern is shown when looking at F_{ST}, although further attention to this gene is needed.

Lastly, *ALX1* is not an outlier in any population. This is interesting since it has been previously shown to be under rapid selection in finches (Lamichhaney et al., 2015). However, based on our genome scan data, it does not seem to play a role in beak size and morphology in these sparrow populations.

Nonetheless, we should keep in mind that, even if these genes have shown to affect beak shape, their effects might be pleiotropic and have other phenotypic effects, which do not involve changes in beak and craniofacial structure.

5. Conclusions

The house sparrow, a human commensal that spread through Europe along with the Neolithic revolution, presents clear differences in skull morphology compared to its ancestral wild non-commensal relative, the Bactrianus sparrow. Skull morphology in Bactrianus appears to be more similar to another wild species, the tree sparrow. These differences are notable in the upper beak, and this might have arisen due to the adaptation of the commensals to larger and harder seeds from cultivated crops. However, further work needs to be done to reveal beak shape changes in more detail. Biting mechanical advantage did not exhibit clear evidence for adaptation to cultivated seeds but more species should be included in this analysis in the future. In an attempt to link form and performance, we suggest studying biomechanics more rigorously in this system, and also fresh tissue such as muscles and ligaments.

Commensal species showed a significantly larger relative brain size, which confirms the hypothesis that larger brains tend to develop when birds face highly variable unpredictable environments, such as urban and agricultural niches. However, more work needs to be done to link this to cognition, such as studies on cognition genes, behaviour and brain structure.

Genomic studies reveal that *TGFB2* and *Col11a1* likely play a key role in the adaptation of commensal sparrows in terms of craniofacial structure. This has helped us to start disentangling the genomic architecture that led the house sparrow to be such a successful commensal. Nonetheless, these and other signatures of selection require a thorough understanding. Future work should aim to look for not only signatures of selection associated with craniofacial morphology but also with feeding habits, cognition and behaviour, and find a link to their gene function.

In conclusion, the European house sparrow shows several evidences for its adaptation to human environments, compared to its ancestral relative (i.e., Bactrianus). Despite more work needs to be done, our findings reveal interesting insights that draw a clearer picture of the origin of commensalism in the house sparrow.

6. References

Abzhanov, A., & Tabin, C. J. (2004). Shh and Fgf8 act synergistically to drive cartilage outgrowth during cranial development. Developmental biology, 273(1), 134-148.

Abzhanov, A., Protas, M., Grant, B. R., Grant, P. R., & Tabin, C. J. (2004). Bmp4 and morphological variation of beaks in Darwin's finches. *Science*, *305*(5689), 1462-1465.

Adams, D. C., Collyer M. L. & Kaliontzopoulou A. (2018). Geomorph: Software for geometric morphometric analyses. R package version 3.0.6.

Adams, D. C., Rohlf, F. J., & Slice, D. E. (2013). A field comes of age: geometric morphometrics in the 21st century. *Hystrix*, *24*(1), 7.

Adler, D. & Murdoch, D. (2018). rgl: 3D Visualization Using OpenGL. R package version 0.99.16.

Allman, J., McLaughlin, T., & Hakeem, A. (1993). Brain weight and life-span in primate species. *Proceedings of the National Academy of Sciences*, *90*(1), 118-122.

Anderson, T. R. (2006). *Biology of the ubiquitous house sparrow: from genes to populations*. Oxford University Press.

Axelsson, E., Ratnakumar, A., Arendt, M. L., Maqbool, K., Webster, M. T., Perloski, M., ... & Lindblad-Toh, K. (2013). The genomic signature of dog domestication reveals adaptation to a starch-rich diet. *Nature*, *495*(7441), 360.

Bock, W. J. (1964). Kinetics of the avian skull. *Journal of Morphology*, *114*(1), 1-41.

Bright, J. A., Marugán-Lobón, J., Cobb, S. N., & Rayfield, E. J. (2016). The shapes of bird beaks are highly controlled by nondietary factors. *Proceedings of the National Academy of Sciences*, *113*(19), 5352-5357.

Brugmann, S. A., Powder, K. E., Young, N. M., Goodnough, L. H., Hahn, S. M., James, A. W., ... & Lovett, M. (2009). Comparative gene expression analysis of avian embryonic facial structures reveals new candidates for human craniofacial disorders. *Human molecular genetics*, *19*(5), 920-930.

Chaves, J. A., Cooper, E. A., Hendry, A. P., Podos, J., De León, L. F., Raeymaekers, J. A., ... & Uy, J. A. C. (2016). Genomic variation at the tips of the adaptive radiation of Darwin's finches. Molecular Ecology, 25(21), 5282-5295.

Chen, S., & Wang, S. (2017). Bird diversities and their responses to urbanization in China. In *Ecology and conservation of birds in urban environments* (pp. 55-74). Springer, Cham.

Cohen, S. B., & Dor, R. (2018). Phenotypic divergence despite low genetic differentiation in house sparrow populations. *Scientific reports*, *8*(1), 394.

Danecek, P., & McCarthy, S. A. (2017). BCFtools/csq: haplotype-aware variant consequences. *Bioinformatics*, *33*(13), 2037-2039.

Danecek, P., Auton, A., Abecasis, G., Albers, C. A., Banks, E., DePristo, M. A., ... & McVean, G. (2011). The variant call format and VCFtools. *Bioinformatics*, *27*(15), 2156-2158.

De León, L. F., Raeymaekers, J. A., Bermingham, E., Podos, J., Herrel, A., & Hendry, A. P. (2011). Exploring possible human influences on the evolution of Darwin's finches. *Evolution: International Journal of Organic Evolution*, *65*(8), 2258-2272.

Deaner, R. O., Isler, K., Burkart, J., & Van Schaik, C. (2007). Overall brain size, and not encephalization quotient, best predicts cognitive ability across non-human primates. *Brain, behavior and evolution*, *70*(2), 115-124.

DePristo, M. A., Banks, E., Poplin, R., Garimella, K. V., Maguire, J. R., Hartl, C., ... & McKenna, A. (2011). A framework for variation discovery and genotyping using next-generation DNA sequencing data. *Nature genetics*, *43*(5), 491.

Ducatez, S., Clavel, J., & Lefebvre, L. (2015). Ecological generalism and behavioural innovation in birds: technical intelligence or the simple incorporation of new foods?. *Journal of Animal Ecology*, *84*(1), 79-89.

Dumont, E. R., Samadevam, K., Grosse, I., Warsi, O. M., Baird, B., & Davalos, L. M. (2014). Selection for mechanical advantage underlies multiple cranial optima in new world leaf-nosed bats. *Evolution*, *68*(5), 1436-1449.

Elgvin, T. O., Trier, C. N., Tørresen, O. K., Hagen, I. J., Lien, S., Nederbragt, A. J., ... & Sætre, G. P. (2017). The genomic mosaicism of hybrid speciation. *Science Advances*, *3*(6), e1602996.

Eroukhmanoff, F., Hermansen, J. S., Bailey, R. I., Sæther, S. A., & Sætre, G. P. (2013). Local adaptation within a hybrid species. *Heredity*, *111*(4), 286.

Falk, D., Cheverud, J., Vannier, M. W., & Conroy, G. C. (1986). Advanced computer graphics technology reveals cortical asymmetry in endocasts of rhesus monkeys. *Folia Primatologica*, *46*(2), 98-103.

Felice, R. N., & Goswami, A. (2018). Developmental origins of mosaic evolution in the avian cranium. *Proceedings of the National Academy of Sciences*, *115*(3), 555-560.

Felice, R. N., Tobias, J. A., Pigot, A. L., & Goswami, A. (2019). Dietary niche and the evolution of cranial morphology in birds. *Proceedings of the Royal Society B*, *286*(1897), 20182677.

Fox, J. & Weisberg, W. (2011). An R Companion to Applied Regression, Second Edition. Thousand Oaks CA: Sage.

Franklin, D. C., Garnett, S. T., Luck, G. W., Gutierrez-Ibanez, C., & Iwaniuk, A. N. (2014). Relative brain size in Australian birds. *Emu*, *114*(2), 160-170.

Fuller, D. Q., & Allaby, R. (2018). Seed dispersal and crop domestication: shattering, germination and seasonality in evolution under cultivation. *Annual Plant Reviews online*, 238-295.

Fuller, D. Q., & Stevens, C. J. (2019). Between domestication and civilization: the role of agriculture and arboriculture in the emergence of the first urban societies. *Vegetation History and Archaeobotany*, *28*(3), 263-282.

Gavrilov, E. I., & Korelov, M. N. (1968). The Indian sparrow as a distinct good species. *Byulleten'Moskovskogo Obshchestva Ispytateleley Prirody Otdel Biologicheskiy*, *73*, 115-122.

Gower, J. C. (1975). Generalized procrustes analysis. *Psychometrika*, *40*(1), 33-51.

Grant, B. R., & Grant, P. R. (1996). High survival of Darwin's finch hybrids: effects of beak morphology and diets. *Ecology*, *77*(2), 500-509.

Grant, P. R., & Grant, B. R. (2002). Unpredictable evolution in a 30-year study of Darwin's finches. *science*, *296*(5568), 707-711.

Griffith, A. J., Sprunger, L. K., Sirko-Osadsa, D. A., Tiller, G. E., Meisler, M. H., & Warman, M. L. (1998). Marshall syndrome associated with a splicing defect at the COL11A1 locus. *The American Journal of Human Genetics*, *62*(4), 816-823.

Guo, H., Xing, Y., Liu, Y., Luo, Y., Deng, F., Yang, T., ... & Li, Y. (2016). Wnt/β-catenin signaling pathway activates melanocyte stem cells in vitro and in vivo. Journal of Dermatological Science, 83(1), 45-51.

Hall, B. K. 1993. The skull: Volume 2, Patterns of structural and systematic diversity.

Healy, S. D., & Rowe, C. (2006). A critique of comparative studies of brain size. *Proceedings of the Royal Society B: Biological Sciences*, *274*(1609), 453-464.

Herrel, A., Podos, J., Huber, S. K., & Hendry, A. P. (2005). Bite performance and morphology in a population of Darwin's finches: implications for the evolution of beak shape. *Functional Ecology*, *19*(1), 43-48.

Hooper, L. V., & Gordon, J. I. (2001). Commensal host-bacterial relationships in the gut. *Science*, *292*(5519), 1115-1118.

Hulme-Beaman, A., Dobney, K., Cucchi, T., & Searle, J. B. (2016). An ecological and evolutionary framework for commensalism in anthropogenic environments. *Trends in Ecology & Evolution*, *31*(8), 633-645.

Husby, A., Hille, S. M., & Visser, M. E. (2011). Testing mechanisms of Bergmann's rule: phenotypic decline but no genetic change in body size in three passerine bird populations. *The American Naturalist*, *178*(2), 202-213.

Iwaniuk, A. N., & Nelson, J. E. (2002). Can endocranial volume be used as an estimate of brain size in birds?. *Canadian Journal of Zoology*, *80*(1), 16-23.

Jensen, H., Sæther, B. E., Ringsby, T. H., Tufto, J., Griffith, S. C., & Ellegren, H. (2003). Sexual variation in heritability and genetic correlations of morphological traits in house sparrow (Passer domesticus). *Journal of evolutionary biology*, *16*(6), 1296-1307.

Jones, E. P., Eager, H. M., Gabriel, S. I., Jóhannesdóttir, F., & Searle, J. B. (2013). Genetic tracking of mice and other bioproxies to infer human history. *Trends in Genetics*, *29*(5), 298-308.

Jones, S., Pfister-Genskow, M., Cirelli, C., & Benca, R. M. (2008). Changes in brain gene expression during migration in the white-crowned sparrow. *Brain research bulletin*, *76*(5), 536-544.

Kark, S., Iwaniuk, A., Schalimtzek, A., & Banker, E. (2007). Living in the city: can anyone become an 'urban exploiter'?. *Journal of Biogeography*, *34*(4), 638-651.

Kendall, D. G. (1977). The diffusion of shape. *Advances in applied probability*, *9*(3), 428-430.

Klingenberg, C. P. (2016). Size, shape, and form: concepts of allometry in geometric morphometrics. *Development genes and evolution*, *226*(3), 113-137.

Kluyver, T. A., Jones, G., Pujol, B., Bennett, C., Mockford, E. J., Charles, M., ... & Osborne, C. P. (2017). Unconscious selection drove seed enlargement in vegetable crops. *Evolution letters*, *1*(2), 64-72.

Krebs, C.J. (2013). *Ecology: Pearson New International Edition: The Experimental Analysis of Distribution and Abundance* 6th edition, Pearson Education Limited.

Kumar, M., Ray, P., & Chapman, S. C. (2012). Fibroblast growth factor and bone morphogenetic protein signaling are required for specifying prechondrogenic identity in neural crest-derived mesenchyme and initiating the chondrogenic program. Developmental Dynamics, 241(6), 1091-1103.

Labocha, M. K., & Hayes, J. P. (2012). Morphometric indices of body condition in birds: a review. *Journal of Ornithology*, *153*(1), 1-22.

Lamichhaney, S., Berglund, J., Almén, M. S., Maqbool, K., Grabherr, M., Martinez-Barrio, A., ... & Grant, B. R. (2015). Evolution of Darwin's finches and their beaks revealed by genome sequencing. *Nature*, *518*(7539), 371.

Larson, G., & Fuller, D. Q. (2014). The evolution of animal domestication. *Annual Review of Ecology, Evolution, and Systematics*, *45*, 115-136.

Lautenschlager, S. (2013). Cranial myology and bite force performance of E rlikosaurus andrewsi: a novel approach for digital muscle reconstructions. *Journal of Anatomy*, *222*(2), 260-272.

Lautenschlager, S., Bright, J. A., & Rayfield, E. J. (2014). Digital dissection–using contrast-enhanced computed tomography scanning to elucidate hard-and soft-tissue anatomy in the Common Buzzard Buteo buteo. *Journal of Anatomy*, *224*(4), 412-431.

Lawson, L. P., & Petren, K. (2017). The adaptive genomic landscape of beak morphology in Darwin's finches. *Molecular ecology*, *26*(19), 4978-4989.

Lefebvre, L., & Nicolakakis, N. (2000). Forebrain size and innovation rate in European birds: feeding, nesting and confounding variables. *Behaviour*, *137*(11), 1415-1429.

Lefebvre, L., Whittle, P., Lascaris, E., & Finkelstein, A. (1997). Feeding innovations and forebrain size in birds. *Animal Behaviour*, *53*(3), 549-560.

Lundregan, S. L., Hagen, I. J., Gohli, J., Niskanen, A. K., Kemppainen, P., Ringsby, T. H., ... & Ranke, P. S. (2018). Inferences of genetic architecture of bill morphology in house sparrow using a high-density SNP array point to a polygenic basis. *Molecular ecology*, *27*(17), 3498-3514.

Maeda, T. (1998). Bird communities and habitat relationships in a residential area of Tokyo. *Journal of the Yamashina Institute for Ornithology*, *30*(2), 83-100.

Maklakov, A. A., Immler, S., Gonzalez-Voyer, A., Rönn, J., & Kolm, N. (2011). Brains and the city: big-brained passerine birds succeed in urban environments. *Biology letters*, *7*(5), 730-732.

Mallarino, R., Campàs, O., Fritz, J. A., Burns, K. J., Weeks, O. G., Brenner, M. P., & Abzhanov, A. (2012). Closely related bird species demonstrate flexibility between beak morphology and underlying developmental programs. *Proceedings of the National Academy of Sciences*, *109*(40), 16222-16227.

Mallarino, R., Grant, P. R., Grant, B. R., Herrel, A., Kuo, W. P., & Abzhanov, A. (2011). Two developmental modules establish 3D beak-shape variation in Darwin's finches. *Proceedings of the National Academy of Sciences*, *108*(10), 4057-4062.

Mann, M., Glickman, S., & Towe, A. (1988). Brain/Body Relations among Myomorph Rodents. Brain, Behavior and Evolution, 31(2), 111-124.

Marino, L. (1998). A Comparison of Encephalization between Odontocete Cetaceans and Anthropoid Primates. *Brain, Behavior and Evolution, 51*(4), 230-238.

Møller, A. P., Díaz, M., Flensted-Jensen, E., Grim, T., Ibáñez-Álamo, J. D., Jokimäki, J., ... & Tryjanowski, P. (2015). Urbanized birds have superior establishment success in novel environments. *Oecologia*, *178*(3), 943-950.

Mougi, A. (2016). The roles of amensalistic and commensalistic interactions in large ecological network stability. *Scientific Reports*, *6*, 29929.

Navalón, G., Bright, J. A., Marugán-Lobón, J., & Rayfield, E. J. (2019). The evolutionary relationship among beak shape, mechanical advantage, and feeding ecology in modern birds. *Evolution*, *73*(3), 422-435.

Nei, M., & Li, W. H. (1979). Mathematical model for studying genetic variation in terms of restriction endonucleases. *Proceedings of the National Academy of Sciences*, *76*(10), 5269-5273.

Noramly, S., Freeman, A., & Morgan, B. A. (1999). Beta-catenin signaling can initiate feather bud development. Development, 126(16), 3509-3521.

Palumbi, S. R. (2001). Humans as the world's greatest evolutionary force. *Science*, *293*(5536), 1786-1790.

Perry, G. H., Dominy, N. J., Claw, K. G., Lee, A. S., Fiegler, H., Redon, R., ... & Carter, N. P. (2007). Diet and the evolution of human amylase gene copy number variation. *Nature genetics*, *39*(10), 1256.

Pfeifer, B., Wittelsbürger, U., Ramos-Onsins, S. E., & Lercher, M. J. (2014). PopGenome: an efficient Swiss army knife for population genomic analyses in R. *Molecular biology and evolution*, *31*(7), 1929-1936.

Piersma, T., & Davidson, N. C. (1991). Confusions of mass and size. *The Auk*, *108*(2), 441-443.

Piñeiro Fernández, L. (2015). Beak shape variation in a hybrid species: effects of diet, insularity and species interactions. Master thesis – CEES, University of Oslo.

Purugganan, M. D., & Fuller, D. Q. (2009). The nature of selection during plant domestication. *Nature*, *457*(7231), 843..

Radinsky, L. (1967). Relative brain size: a new measure. *Science*, *155*(3764), 836-838.

Ravinet, M., Elgvin, T. O., Trier, C., Aliabadian, M., Gavrilov, A., & Sætre, G. P. (2018). Signatures of human-commensalism in the house sparrow genome. *Proceedings of the Royal Society B: Biological Sciences*, *285*(1884), 20181246.

Rehkämper, G., Schuchmann, K., Schleicher, A., & Zilles, K. (1991). Encephalization in Hummingbirds (Trochilidae). *Brain, Behavior and Evolution*, *37*(2), 85-91.

Reznick, D. N., & Ghalambor, C. K. (2001). The population ecology of contemporary adaptations: what empirical studies reveal about the conditions that promote adaptive evolution. *Genetica*, *112*(1), 183-198.

Rising, J. D., & Somers, K. M. (1989). The measurement of overall body size in birds. *The Auk*, *106*(4), 666-674.

Rivera-Pérez, J. A., Wakamiya, M., & Behringer, R. R. (1999). Goosecoid acts cell autonomously in mesenchyme-derived tissues during craniofacial development. Development, 126(17), 3811-3821.

Riyahi, S., Hammer, Ø., Arbabi, T., Sánchez, A., Roselaar, C. S., Aliabadian, M., & Sætre, G. P. (2013). Beak and skull shapes of human commensal and non-commensal house sparrows Passer domesticus. *BMC Evolutionary Biology*, *13*(1), 200.

Rosza, L., Gaxiola, A., Lefebvre, L., Timmermans, S., Dawson, S., & Kabai, P. (1998). Feeding innovations and forebrain size in Australasian birds. *Behaviour*, *135*(8), 1077-1097.

Rowe, A., Richman, J. M., & Brickell, P. M. (1991). Retinoic acid treatment alters the distribution of retinoic acid receptor-beta transcripts in the embryonic chick face. Development, 111(4), 1007-1016.

Runemark, A., Trier, C. N., Eroukhmanoff, F., Hermansen, J. S., Matschiner, M., Ravinet, M., ... & Saetre, G. P. (2018). Variation and constraints in hybrid genome formation. *Nature ecology & evolution*, *2*(3), 549.

Sætre, G. P., Cuevas, A., Hermansen, J. S., Elgvin, T. O., Fernández, L. P., Sæther, S. A., ... & Eroukhmanoff, F. (2017). Rapid polygenic response to secondary contact in a hybrid species. *Proceedings of the Royal Society B: Biological Sciences*, *284*(1853), 20170365.

Sætre, G. P., Riyahi, S., Aliabadian, M., Hermansen, J. S., Hogner, S., Olsson, U., ... & Elgvin, T. O. (2012). Single origin of human commensalism in the house sparrow. *Journal of Evolutionary Biology*, *25*(4), 788-796.

Sakamoto, M. (2010). Jaw biomechanics and the evolution of biting performance in theropod dinosaurs. *Proceedings of the Royal Society B: Biological Sciences*, *277*(1698), 3327-3333.

Santini, L., González-Suárez, M., Russo, D., Gonzalez-Voyer, A., von Hardenberg, A., & Ancillotto, L. (2019). One strategy does not fit all: determinants of urban adaptation in mammals. *Ecology letters*, *22*(2), 365-376.

Sayol, F., Downing, P. A., Iwaniuk, A. N., Maspons, J., & Sol, D. (2018). Predictable evolution towards larger brains in birds colonizing oceanic islands. *Nature communications*, *9*(1), 2820.

Sayol, F., Maspons, J., Lapiedra, O., Iwaniuk, A. N., Székely, T., & Sol, D. (2016). Environmental variation and the evolution of large brains in birds. *Nature Communications*, *7*, 13971.

Searle, J. B., Jones, C. S., Gündüz, İ., Scascitelli, M., Jones, E. P., Herman, J. S., ... & Jóhannesdóttir, F. (2008). Of mice and (Viking?) men: phylogeography of British and Irish house mice. *Proceedings of the Royal Society B: Biological Sciences*, *276*(1655), 201-207.

Sol, D. (2008). Revisiting the cognitive buffer hypothesis for the evolution of large brains. *Biology letters*, *5*(1), 130-133.

Sol, D., Duncan, R. P., Blackburn, T. M., Cassey, P., & Lefebvre, L. (2008). Big brains, enhanced cognition, and response of birds to novel environments. *Proceedings of the National Academy of Sciences*, *102*(15), 5460-5465.

Sol, D., Lefebvre, L., & Rodríguez-Teijeiro, J. D. (2005). Brain size, innovative propensity and migratory behaviour in temperate Palaearctic birds. *Proceedings of the Royal Society B: Biological Sciences*, *272*(1571), 1433-1441.

Sol, D., Sayol, F., Ducatez, S., & Lefebvre, L. (2016). The life-history basis of behavioural innovations. *Philosophical Transactions of the Royal Society B: Biological Sciences*, *371*(1690), 20150187.

Soons, J., Herrel, A., Genbrugge, A., Adriaens, D., Aerts, P., & Dirckx, J. (2012). Multi-layered bird beaks: a finite-element approach towards the role of keratin in stress dissipation. *Journal of the Royal Society Interface*, *9*(73), 1787-1796.

Soons, J., Herrel, A., Genbrugge, A., Aerts, P., Podos, J., Adriaens, D., ... & Dirckx, J. (2010). Mechanical stress, fracture risk and beak evolution in Darwin's ground finches (Geospiza). *Philosophical Transactions of the Royal Society B: Biological Sciences*, *365*(1543), 1093-1098.

Summers-Smith, J. D. (1963). *The house sparrow* (pp. 149-159). London: Collins.

Summers-Smith, J. D. (1988). The Sparrows: A study of the genus. *Passer. T & AD Poyser, Staffordshire, England*.

Tajima, F. (1989). Statistical method for testing the neutral mutation hypothesis by DNA polymorphism. *Genetics*, *123*(3), 585-595.

Terai, Y., Morikawa, N., & Okada, N. (2002). The evolution of the pro-domain of bone morphogenetic protein 4 (Bmp4) in an explosively speciated lineage of East African cichlid fishes. *Molecular Biology and Evolution*, *19*(9), 1628-1632.

Tokita, M., Yano, W., James, H. F., & Abzhanov, A. (2017). Cranial shape evolution in adaptive radiations of birds: comparative morphometrics of Darwin's finches and Hawaiian honeycreepers. *Philosophical Transactions of the Royal Society B: Biological Sciences*, *372*(1713), 20150481.

Uz, E., Alanay, Y., Aktas, D., Vargel, I., Gucer, S., Tuncbilek, G., ... & Ozdag, H. (2010). Disruption of ALX1 causes extreme microphthalmia and severe facial clefting: expanding the spectrum of autosomal-recessive ALX-related frontonasal dysplasia. *The American Journal of Human Genetics*, *86*(5), 789-796.

Van der Meij, M. A. A., & Bout, R. G. (2004). Scaling of jaw muscle size and maximal bite force in finches. *Journal of Experimental Biology*, *207*(16), 2745-2753.

Van der Meij, M. A. A., & Bout, R. G. (2006). Seed husking time and maximal bite force in finches. *Journal of Experimental Biology*, *209*(17), 3329-3335.

Vaurie, C. (1956). Systematic notes on Palearctic birds. No. 24, Ploceidae, the genera Passer, Petronia, and Montifringilla. American Museum novitates; no. 1814.

Vincze, O. (2016). Light enough to travel or wise enough to stay? Brain size evolution and migratory behavior in birds. *Evolution*, *70*(9), 2123-2133.

Weir, B. S., & Cockerham, C. C. (1984). Estimating F-statistics for the analysis of population structure. *Evolution*, *38*(6), 1358-1370.

Westneat, M. W. (1994). Transmission of force and velocity in the feeding mechanisms of labrid fishes (Teleostei, Perciformes). *Zoomorphology*, *114*(2), 103-118.

Wu, X., Walker, J., Zhang, J., Ding, S., & Schultz, P. G. (2004). Purmorphamine induces osteogenesis by activation of the hedgehog signaling pathway. Chemistry & biology, 11(9), 1229-1238.

Zelditch, M., Swiderski, D., Sheets, D. H., & Fink, W. L. (2004). Geometric morphometrics for biologists: A primer: Elsevier Academic Press. *Waltham, MA*.

Zusi, R. L. (1993). Patterns of diversity in the avian skull. *The skull*, *2*, 391-437.

7. Appendix

A1. Landmarks definition

1. The tip of the upper beak
2. The maximum curvature at the rostral end of the external nares
3. The maximum curvature at the dorsal end of the external nares
4. The maximum curvature at the caudal end of the external nares
5. The most lateral point at the processus antorbitalis
6. The most dorso-caudal point at the processus supraorbitalis
7. The point where the esquamosalis process meets the squamosal
8. Most caudal point of the fosa temporalis that meets the crista temporalis
9. Insertion point of the processus suprameaticus of the quadrate bone
10. The point where the most rostro-lateral edge of the jugal bar meets the upper beak (the processus maxilaris praemaxillae)
11. The most caudal point of the vomer
12. The most rostral point of the projection of the parasphenoid.
13. The subsidence just anterior to the condilus occipitalis
14. Midline of the craniofacial hinge.
15. The projection on the dorsal view of the sagittal plane of the meeting point between the most anterior point of both orbits (see fig A1)
16. The projection on the dorsal view of the sagittal plane of the meeting point between the pterygoids (see fig A1).
17. Intersection point between the parietal and frontal bone on the sagittal plane (see fig A1).
18. Most dorsal midpoint between 2 and its mirrored landmark on the left side when looking at the dorsal view.
19. Most dorsal midpoint between 3 and its mirrored landmark on the left side when looking at the dorsal view.
20. Most caudal point at the occipital crest

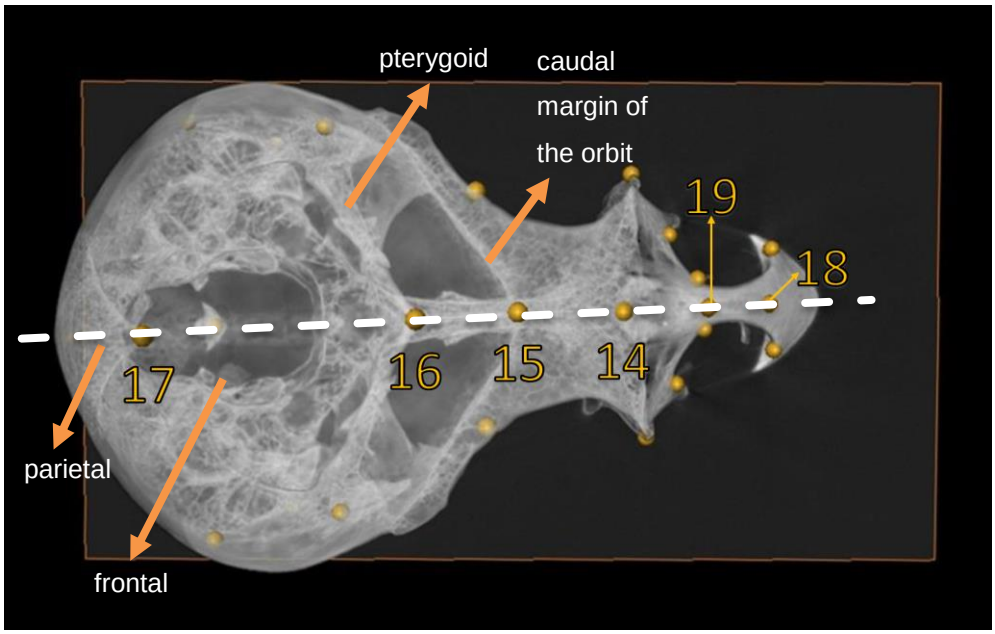

Figure A1. Representation of landmarks 14-19 in a sparrow skull, using the orthoslice in Avizo and lowering the alpha values to change the transparency of the scan. White dashed line represents the sagittal plane.

A2. Validation of methods

Correlation test between endocranial volume measured with filling the skull with mustard seeds and with a 3D reconstruction.

We used Pearson's product-moment correlation with the base R function *cor.test().*

Table A2. Correlation test between measurements of braincase volume with two different methods. 'cor' stands for Pearson's product-moment correlation.

t	df	p-value	95% CI	cor
9.5451	12	5.908×10^{-07}	(0.8168190, 0.9812107)	0.94

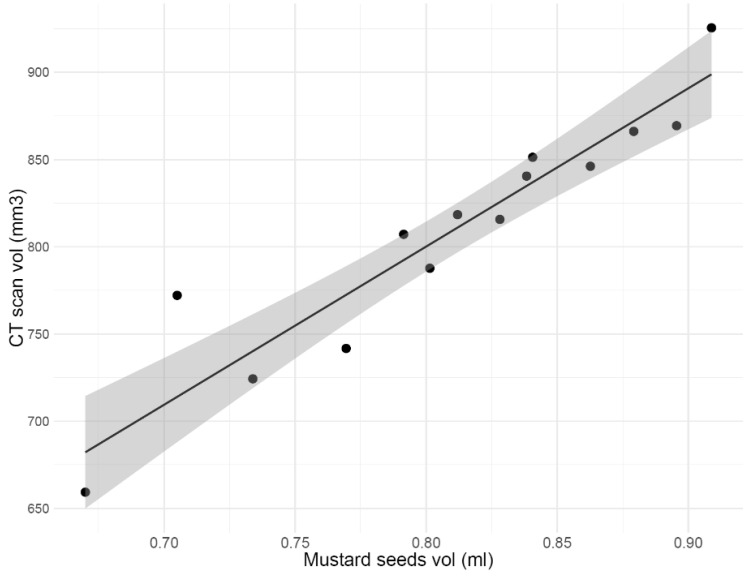

Figure A2. Regression between measurements taken with both methods. On the x axes, the volume obtained with mustard seeds, converted to ml. On the Y axis the resulting brain volume from the 3D reconstruction out of CTscans. Shading represents standard deviation.

A3. Tables 50 candidate genes

Genes previously associated with bill morphology in Darwin's finches				
Gene		**Chr**	**Function**	**Literature**
ALX1	ALX homeobox 1 (*Homo sapiens*)	1A	Craniofacial development mesenchyme and the first pharyngeal arch. Associated with blunt beaks.	Lamichhaney 2015; Uz et al., 2010
BMP4	Bone morphogenetic protein 4 (*Gallus gallus)*	5	Development of prenasal cartilage. Expression upregulated for deeper and wider beaks.	Abzhanov et al., 2004; Mallarino et al., 2011
CALM1	Calmodulin (*Xenopus laevis*)	3	Development of prenasal cartilage. Expression upregulated for longer beaks.	Mallarino et al., 2011
CTNNB1	Catenin beta-1 (*Canis familiaris*)	2	Development of premaxillary bone. Expression upregulated for longer and deeper beaks..	Abzhanov et al., 2006; Mallarino et al., 2011
DKK2	Dickkopf Wnt singalling pathway inhibitor 2 (*Homo sapiens*)	4	Upregulation of Wnt pathway leads to wider bills.	Brugmann et al., 2009
DKK3	Dickkopf related protein 3 (*Gallus gallus*)	5	Development of premaxillary bone. Expression upregulated for longer and deeper beaks..	Mallarino 2012
DLK1	Protein delta homolog 1 (*Homo sapiens*)	5	Beak shape and size diversification across Darwin's finches clade.	Lamichhaney et al., 2015; Chaves et al 2016
FGF8	Fibroblast growth factor 8 (*Gallus gallus*)	6	Development of the frontonasal ectoderm. Shh pathway for BMP4 expression. Expression in pharyngeal endoderm	Abzhanov & Tabin 2004; Wu et al 2004; Kumar, Ray & Champman 2012
FGF10	Fibroblast growth factor 10 (*Homo sapiens*)	Z	Craniofacial development.	Brugmann et al., 2009; Lamichhaney et al., 2015
FGF19	Fibroblast growth factor 19 (*Homo sapiens*)	5	Strong expression in pharyngeal endoderm. Formation of columella mesenchyme.	Haworth et al 2004; Kumar, Ray & Champman 2012
FZD1	Frizzled-1 (*Gallus gallus*)	2	Upregulation of Wnt pathway leads to wider bills.	Brugmann et al., 2009
GSC	Homeobox protein goosecoid (*Gallus gallus*)	5	Acts on mesenchyme-derived tissues during craniofacial development	Rivera-Pérez, Wakamiya & Behringer, 1999; Lamichhaney et al., 2015
HMGA1	High mobility AT-hook 2 (*Homo sapiens*)	1A	Beak shape and size diversification across Darwin's finches clade.	Lamichhaney et al., 2015; Chaves et al 2016
RDH14	Retinol dehydrogenase 14 (*Homo sapiens*)	3	Abnormalities during craniofacial development. Inhibition of development of frontonasal structures.	Rowe, Richman & Brickell, 1991; Lamichhaney et al., 2015
SHH	Sonic hedgehog (*Gallus gallus*)	2	Development of the frontonasal ectoderm. Upregulation for BMP4 expression.	Abzhanov & Tabin 2004; Wu et al 2004
TGFbIIr	Transforming growth factor beta receptor type II (*Gallus gallus*)	7	Development of premaxillary bone. Expression upregulated for longer and deeper beaks..	Mallarino et al., 2011

High *Fst* between *Geosiza fortis* and *G. scandens* (Darwin's finches) (Lawson & Petren, 2017)

Gene		Chr
Related to bone growth, joints, skin, keratin		
EXT1	Exostosin-1 (*Cricetulus griseus*)	2
Related to macrodontia of permanent maxillary central incisor, cleft secondary palate, abnormal head morphology, abnormal palate morphology		
GJA1	Gap junction alpha-1 protein (*Gallus gallus*)	3
VPS13Ba	Vacuolar protein sorting-associated protein 13B (*Homo sapiens*)	2
VPS13Bb	Vacuolar protein sorting-associated protein 13B (*Homo sapiens*)	2
Related to nasal eminence, mandibular/maxillary arch, paraxial mesoderm, epithelium, mesenchyme and olfactory pit		
ATXN1	ALX homeobox protein 1 (*Homo sapiens*)	1A
DKGBa	Diacylglycerol kinase beta (*Homo sapiens*)	9
DKGBb	Diacylglycerol kinase beta (*Homo sapiens*)	2
HMGA2	High mobility group protein HMGI-C (*Homo sapiens*)	1A
LAMA2	Laminin subunit alpha-2 (*Homo sapiens)*	3
MGAT4Ca	Alpha-1,2,C3-mannosyl-glycoprotein 4-beta-N-acetylglucosaminyltransferase C (*Gallus gallus*)	26
MGAT4Cb	Alpha-1,2,C3-mannosyl-glycoprotein 4-beta-N-acetylglucosaminyltransferase C (*Macaca fascicularis*)	1A
PDE10A	cAMP and cAMP-inhibited cGMP 3'%2C5'-cyclic phosphodiesterase 10A (*Homo sapiens*)	3
PTPRJ	Receptor-type tyrosine-protein phosphatase eta (*Gallus gallus*)	5
SEMA5A	Semaphorin-5A (*Homo sapiens*)	2
SH3PXD2A	SH3 and PX domain-containing protein 2A (*Homo sapiens*)	6
SIX2	Homeobox protein SIX2 (*Mus musculus*)	3
TES	Testin (*Gallus gallus*)	1A
THBS2	Thrombospondin-2 (*Gallus gallus*)	3
RASSF9	Ras association domain-containing protein 9 (*Homo sapiens*)	1A

Genes associated with signatures of selection for human commensalism in the house sparrow (*P. domesticus*) (Ravinet et al., 2018)

Gene		Chr	Function
AMY2A	Pancreatic alpha-amylase (*Homo sapiens*)	8	Linked to a shift to starch-based diet in humans and dogs (Perry et al., 2007; Axelsson et al., 2013)
COL11A1a	Collagen alpha-1(XI) chain (*Mus musculu* s)	17	Regulates craniofacial and skull development. Associated with Marshall's syndrome in humans (skull thickness and abnormal facial structure Griffith et al., 1988))
COL11A1b	Collagen alpha-1(XI) chain (*Mus musculus*)	8	Regulates craniofacial and skull development. Associated with Marshall's syndrome in humans (skull thickness and abnormal facial structure (Griffith et al., 1988))
COL11A1c	Collagen alpha-1(XI) chain (*Mus musculus*)	8	Regulates craniofacial and skull development. Associated with Marshall's syndrome in humans (skull thickness and abnormal facial structure (Griffith et al., 1988))
PARL	Presenilins-associated rhomboid-like proteinmitochondrial (*Bos taurus*)	9	Upregulated during migration in white-crowned sparrows (Jones et al., 2008)
WNT7A	Protein Wnt-7a (*Mus musculus*)	12	Feather development and melanogenesis in birds (Guo et al., 2016; Noramly, Freeman & Morgan, 1999)

Flanking genes for significant markers associated with bill morphology on house sparrow (*P. domesticus)* (Lundregan et al., 2018)

Gene		Chr	Effect on:
Bmpk2	BMP-2-inducible protein kinase (*Homo sapiens*)	4	Bill length
CBLB	E3 ubiquitin-protein ligase CBL-B (*Homo sapiens*)	1	Bill length
CEBPZ	E3 ubiquitin-protein ligase CBL-B (*Homo sapiens*)	3	Bill depth
Glis1	Zinc finger protein GLIS1 (*Homo sapiens*)	8	Bill length
MAOA	Amine oxidase [flavin-containing] A (*Equus caballus*)	1	Bill length
NFIA	Nuclear factor 1 A-type (*Gallus gallus*)	8	Bill length

A4. PCA: variance contributions, scree plot and PCA without allometry correction

3D morphometrics. Allometry corrected PCA scree plot and table of explained variation for the first ten dimensions.

Table A.4.1 Percentage of variance explained by the first 10 axes of variance in the allometry-free PCA. Total %explained variance in first 10 dimensions = 74.92.

Eigenvector	% explained variance
1	16.15
2	12.83
3	9.85
4	8.61
5	6.03
6	5.70
7	4.75
8	4.49
9	3.62
10	2.88

Figure A.4.1 Scree plot of the percentage of variance explained by each dimension in the allometry-corrected PCA.

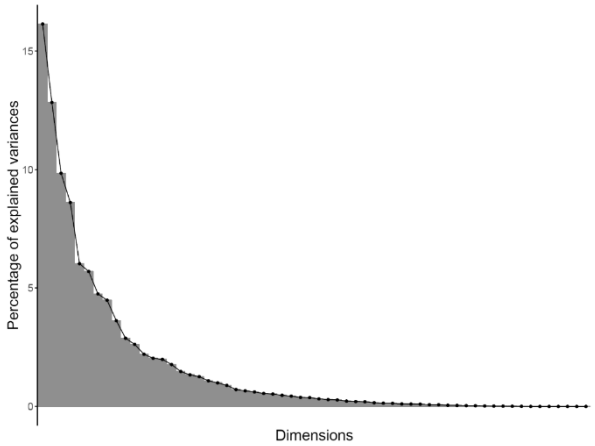

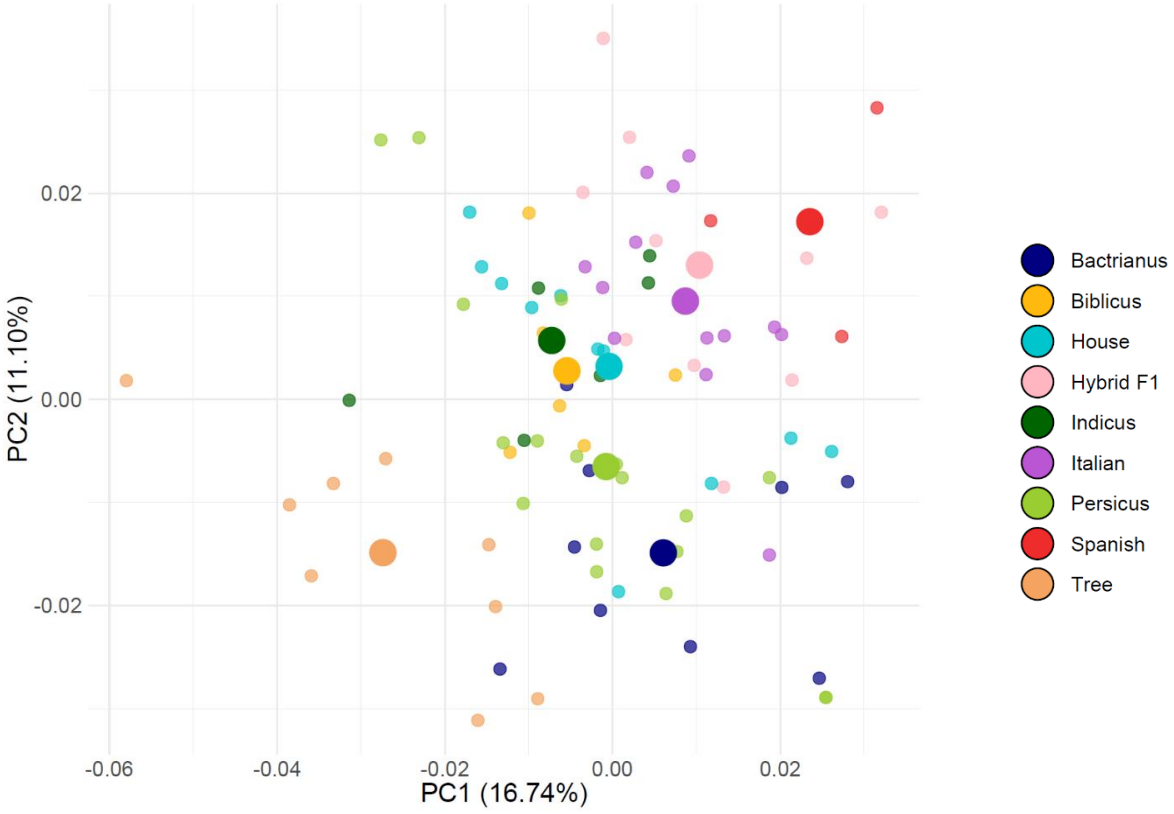

Figure A4.2. (a) PCA on raw Procrustes distances (no allometry correction) showing species distribution along PC1 and PC2 for skull shape variation. Each point represents one individual. Large points represent mean shape per group (i.e. species or subspecies). Percentage of explained variance on PC1 is slightly higher than in the allometry corrected PCA, and PC2 is slightly lower.

Table A4.2 Percentage of variance explained by the first 10 axes of variance in the raw PCA (fig. A4.2). Total %explained variance in first 10 dimensions = 73.52

Eigenvector	% explained variance
1	16.74
2	11.10
3	9.59
4	7.05
5	6.43
6	5.77
7	5.12
8	4.59
9	3.98
10	3.15

Figure A4.3 Scree plot of the percentage of variance explained by each dimension in the raw PCA on Procrustes data (fig. A4.2).

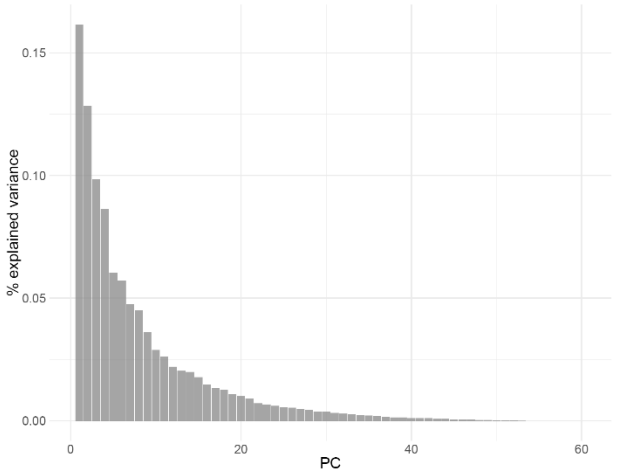

Table A4.3 Multivariate analysis of variance on group differences for the first 10 dimensions. The grouping variable 'Species' shows that there're effectively significant differences in shape for the different groups when comparing PC values of the morphospace. Signif. codes: 0 '***' 0.001 '**' 0.01 '*' 0.05 '.' 0.1 ' ' 1

	Df	Pillai	Aprox F	Num Df	Den Df	Pr (>F)
Intercept	1	0.000	0.0000	10	68	1
Species	8	2.177	2.8039	80	600	1.368×10^{-12} ***
Residuals	77					

A5. Centroid sizes

Table A5.1 ANOVA on skull centroid sizes (including all 20 landmarks). Signif. codes: 0 '***' 0.001 '**' 0.01 '*' 0.05 '.' 0.1 ' ' 1

	Df	Sum Sq	Mean Sq	F value	Pr(>F)
Species	8	191.40	23.925	41.18	$<2x10^{-16}$***
Residuals	77	41.18	0.581		

Table A5.2 Post-hoc pairwise t-test on centroid size (including 20 landmarks). P value adjustment method: "fdr" (BH, Benjamini&Hochberg).

	Bactr	Bibl	House	F1Hyb	Indicus	Italian	Persicus	Spanish
Bibl	2.2e-13							
House	2.1e-12	0.08200						
F1Hyb	4.4e-11	0.03250	0.62171					
Indicus	7.1e-08	0.01213	0.27360	0.50813				
Italian	2.4e-13	0.10658	0.83825	0.48264	0.19626			
Persicus	8.9e-10	9.6e-08	8.9e-06	0.00013	0.01388	1.2e-06		
Spanish	1.5e-09	0.86023	0.23919	0.13404	0.06089	0.27776	6.7e-05	
Tree	0.00161	<2.e-16	<2e-16	<2e-16	2.0e-13	< 2e-16	5.3e-13	7.3e-14

Table A5.3 ANOVA on beak centroid sizes. Signif. codes: 0 '***' 0.001 '**' 0.01 '*' 0.05 '.' 0.1 ' ' 1

	Df	Sum Sq	Mean Sq	F value	Pr(>F)
Species	8	43.31	5.413	35.27	$<2x10^{-16}$***
Residuals	77	11.82	0.153		

Table A5.4 Post-hoc pairwise t-test on beak centroid size only. P value adjustment method: "fdr" (BH, Benjamini&Hochberg).

	Bactr	Bibl	House	F1Hyb	Indicus	Italian	Persicus	Spanish
Bibl	5.5e-11							
House	1.9e-08	0.02382						
F1Hyb	2.8e-10	0.19547	0.26331					
Indicus	0.00016	0.00158	0.19253	0.02416				
Italian	6.6e-12	0.33552	0.09734	0.61866	0.00587			
Persicus	0.00056	5.9e-07	0.0069	1.0e-05	0.19470	1.8e-07		
Spanish	3.3e-08	0.01655	0.06261	0.26331	0.00719	0.38854	7.7e-05	
Tree	0.00055	<2.e-16	1.2e-15	1.2e-15	2.5e-10	< 2e-16	1.8e-11	5.6e-13

Table A5.5 ANOVA on skull centroid sizes (excluding beak landmarks). Signif. codes: 0 '***' 0.001 '**' 0.01 '*' 0.05 '.' 0.1 ' ' 1

	Df	Sum Sq	Mean Sq	F value	Pr(>F)
Species	8	48.80	6.100	31.38	$<2x10^{-16}$***
Residuals	77	14.97	0.194		

Table A5.6 Post-hoc pairwise t-test on skull centroid sizes (excluding beak landmarks). P value adjustment method: "fdr" (BH, Benjamini&Hochberg).

	Bactr	Bibl	House	F1Hyb	Indicus	Italian	Persicus	Spanish
Bibl	1.7e-11							
House	2.3e-11	0.21870						
F1Hyb	7.0e-09	0.02507	0.21870					
Indicus	3.9e-05	0.00193	0.02353	0.21870				
Italian	3.9e-10	0.03514	0.30107	0.75728	0.13854			
Persicus	0.00013	5.6e-07	3.6e-06	0.00110	0.17687	0.00013		
Spanish	1.5e-07	0.63571	0.63571	0.21506	0.03697	0.25058	0.00072	
Tree	0.00675	3.6e-16	<2.e-16	2.7e-14	9.6e-10	7.6e-16	1.8e-10	2,7e-11

Table A5.7 Linear regression between beak size and vault size. Residual standard error: 0.4302 on 84 degrees of freedom. Multiple R-squared: 0.7179, Adjusted R-squared: 0.7146, F-statistic: 213.8 on 1 and 84 DF, p-value: < 2.2e-16. Signif. codes: 0 '***' 0.001 '**' 0.01 '*' 0.05 '.' 0.1 ' ' 1

	Estimate	Std error	T value	Pr(>|t|)
Intercept	-6.46271	1.28664	-5.023	$2.82x10^{-06}$ ***
Vault	0.78781	0.05388	14.622	$< 2x10^{-16}$ ***

A6. Biting mechanical advantage

Figure A6. Density plot of pooled biting MA calculations for 26 samples of Spanish, Italian, House and F1 Hybrid.

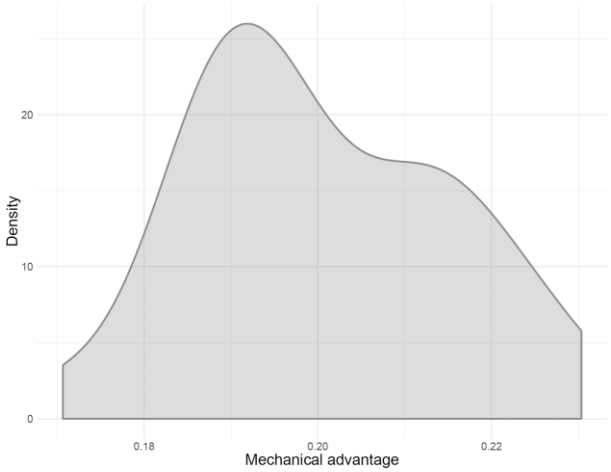

A7. Braincase volume pairwise test

Table A7. Post-hoc pairwise t-test on the residuals of the linear regression *braincase volume ~ tarsus length*. P value adjustment method: fdr (BH, Benjamini&Hochberg).

	Bactr	Bibl	F1 hyb	House	Indicus	Italian	Persic	Spanish
Bibl	4.3e-06							
F1 hyb	0.0624	0.0272						
House	0.0080	0.0890	1.0000					
Indicus	1.0000	0.1483	1.0000	1.0000				
Italian	0.2256	0.0075	1.0000	1.0000	1.0000			
Persic	0.0746	0.0062	1.0000	1.0000	1.0000	1.0000		
Spanish	0.1701	1.0000	1.0000	1.0000	1.0000	1.0000	1.0000	
Tree	1.0000	4.3e-06	0.0624	0.0080	1.0000	0.2256	0.0746	0.1701

A8. Tajima's D linear model and post-hoc pairwise t-test

Table A8.1 Chosen linear model for Tajima's D values, explained by gene status and populations: *Tajima's D ~ population + gene status*, with pop = Bactrianus and status = candidate genes set as the intercept. adj. $R^2 = 0.121$; $F_{7, 679} = 14.49$; p-value = $<2.2x10^{-6}$ Signif. codes: 0 '***' 0.001 '**' 0.01 '*' 0.05 '.' 0.1 ' ' 1

	Estimate	Std. error	t value	Pr(|>t|)
Bact + cand (int)	-0.92227	0.07513	-12.276	< 2e-16 ***
pop biblicus	0.46569	0.09946	4.682	3.42e-06 ***
pop house	0.69940	0.09946	7.032	4.97e-12 ***
pop indicus	0.52348	0.09920	5.277	1.77e-07 ***
pop italian	0.62051	0.09971	6.223	8.54e-10 ***
pop persicus	0.40718	0.09920	4.104	4.55e-05 ***
pop spanish	0.12977	0.09971	1.301	0.194
status null	0.25168	0.05327	4.725	2.80e-06 ***

Table A8.2 Post-hoc pairwise t-test on Tajima's D, with pooled SD. P value adjustment method: fdr (BH, Benjamini&Hochberg).

	Bactrianus	Biblicus	House	Indicus	Italian	Persicus
Biblicus	1.6e-05					
House	2.0e-10	0.03727				
Indicus	1.4e-06	0.57617	0.11967			
Italian	1.4e-08	0.17431	0.49195	0.37966		
Persicus	0.00018	0.57617	0.00794	0.30727	0.05382	
Spanish	0.26296	0.00220	1.9e-07	0.00029	6.5e-06	0.01207